Supporting Information

Pore-Wall Functionalization of Covalent Organic Framework Palladium Catalysts Boosts the Multicomponent Reaction of CO_2

Shiyuan Wei,[1] Benling Yu,[1] Jiawei Li,*[1] Jianhui Zhu,[1] You Wang,[1] Yaqi Li,[1] Jianhan Huang,*[1] You-Nian Liu[1]

[1] College of Chemistry and Chemical Engineering, Hunan Provincial Key Laboratory of Micro and Nano Material Interface Science, Central South University, Changsha 410083, Hunan (P. R. China)

E-mail: lijiawei@csu.edu.cn; jianhanhuang@csu.edu.cn

1. Experimental Procedures

General Materials and Measurements

All of the reagents were commercially available and were used without further purification. Powder X-ray diffraction (PXRD) patterns were collected on an Advance D8 equipped with Ni-filtered Cu K radiation (40 kV, 100 mA) at room temperature with a scan speed of 10 °·min^{-1}. ^{1}H NMR and ^{13}C NMR spectra were done on a Bruker Model AM-400 (400 MHz) spectrometer. Infrared (IR) spectra were measured from a KBr pellets on Nicolet iN10 MX microscopic infrared spectrometer (Thermo Scientific Co., USA) in the range of 4000 to 400 cm^{-1} under ambient condition. The content of metal ions was determined by the inductively coupled plasma mass spectrometry (ICP-MS). The pore structure of the materials was measured by N_2 adsorption-desorption isotherms at 77 K with Micromeritics ASAP 2460 surface area. The S_{BET} of the polymers was calculated using the BET model in the ranging of P/P_0 = 0.05 - 0.30, the total pore volume (V-total) of the materials was calculated from the isotherms at P/P_0 = 0.99, the pore size distribution (PSD), micropore area (S-micro), and V-micro were all calculated by the non-local density functional theory (NLDFT) method. The X-ray photoelectron spectroscopy (XPS) experiments were conducted using Thermo ESCALAB spectrometer with an Al K-α source. Scanning electron microscopy (SEM) measurements were performed on a JSM-7610FPlus microscope at an acceleration voltage of 10 kV.

Synthesis of COF-TA [1]: Typically, a mixture of 1,3,5-Tris(4-aminophenyl)benzene (TAPB) (0.08 mmol, 28.12 mg), terephthalaldehyde (DFB) (0.12 mmol, 16.1 mg), O-DCB (0.5 mL) and n-Butanol (0.5 mL) were added to a 5 mL ampoule and sonicated for 30 min. Then, 6 M HOAc (0.1 ml) was added and sonicated for 5 min. The ampoule containing the mixture was frozen in liquid nitrogen, and after three cycles of freezing-extraction-thawing, the reaction was heated at 120 °C for 72 h. After the reaction was completed, the sample bottle was taken out, cooled to room temperature, transferred to a centrifuge tube, and washed with methanol and THF for 3 times, and then dispersed the solids in 15 mL of saturated NH_4HCO_3, sonicated until uniformly dispersed. The solid was separated after stirring for 4 h. 5 mL of isopropanol was added, and after separation and vacuum drying at 100 ℃ for 12 h, COF-TA was obtained with a yield of 89%.

Synthesis of COF-TA-4F [2]: Typically, a mixture of 1,3,5-Tris(4-aminophenyl)benzene (28.12 mg, 0.08 mmol), 2,3,5,6-Tetrafluoroterephthalaldehyde (24.73 mg, 0.12 mmol), 1,4-dioxane (1.6 mL) and mesitylene (0.4 mL) were added to a 5 mL ampoule and sonicated for 30 min. Then, 6 M HOAc (0.2 ml) was added and sonicated for 5 min. The ampoule containing the mixture was frozen in liquid nitrogen, and after three cycles of freezing-extraction-thawing, the reaction was heated at 120 °C for 72 h. The solid was collected by centrifugation, washed three times with MeOH, THF and CH_2Cl_2, extracted by Soxhlet extraction for one day, and dried overnight under vacuum. Orange powder was obtained in a yield of 85%.

Synthesis of COF-TA-OCH_3 [2]: Typically, a mixture of 1,3,5-Tris(4-

aminophenyl)benzene (28.12 mg, 0.08 mmol), 2,5-dimethoxybenzaldehyde (23.31 mg, 0.12 mmol), 1,4-dioxane (1.6 mL) and mesitylene (0.4 mL) were added to a 5 mL ampoule and sonicated for 30 min. Then, 6 M HOAc (0.2 ml) was added and sonicated for 5 min. The ampoule containing the mixture was frozen in liquid nitrogen, and after three cycles of freezing-extraction-thawing, the reaction was heated at 120 °C for 72 h. The solid was collected by centrifugation, washed three times with MeOH, THF and CH_2Cl_2, extracted by Soxhlet extraction for one day, and dried overnight under vacuum. Yellow powder was obtained in a yield of 86%.

Synthesis of COF-TA-OHex [3]: Typically, a mixture of 1,3,5-Tris(4-aminophenyl)benzene (28.12 mg, 0.08 mmol), 2,5-Bis(hexyloxy)terephthalaldehyde (40.13 mg, 0.12 mmol), 1,4-dioxane (1.6 mL) and mesitylene (0.4 mL) were added to a 5 mL ampoule and sonicated for 30 min. Then, 6 M HOAc (0.2 ml) was added and sonicated for 5 min. The ampoule containing the mixture was frozen in liquid nitrogen, and after three cycles of freezing-extraction-thawing, the reaction was heated at 120 °C for 72 h. The solid was collected by centrifugation, washed three times with MeOH, THF and CH_2Cl_2, extracted by Soxhlet extraction for one day, and dried overnight under vacuum. Yellow powder was obtained in a yield of 89%.

Synthesis of Pd@ TA: The activated COF-TA (30 mg) was dispersed into acetonitrile (4 mL) and sonicated for 30 min. Then $Pd(OAc)_2$ (10 mg) was added. The mixture was heated at 50 ºC for 12 h. The resulting precipitate was collected by centrifugation and washed with acetonitrile four times. The dried solid was dispersed into acetone (2 mL) and $NaBH_4$ solution (2 mL, 4 mg/mL) was added quickly under an ice-water bath, and

the reaction was carried out for 12 h. At the end of the reaction, grey-green powder was obtained, and the solid was washed thoroughly with acetone and water and dried in a vacuum drying oven at 80 °C overnight.

Synthesis of Pd@TA-4F, Pd@TA-OCH_3 and Pd@TA-OHex: As a comparison, Pd@TA-4F, Pd@TA-OCH_3 and Pd@TA-OHex were also synthesized using the same procedure except for the replacement of COF-TA by COF-TA-4F, COF-TA-OCH_3 or COF-TA-OHex, respectively.

Synthesis of poly(N-vinyl-2-pyrrolidone) (PVP) stabilized Pd NPs.

In a round bottle, aqueous Na_2PdCl_4 solution (1.0×10^{-4} mol·cm^{-3}) was added to a preheated (90 °C) aqueous mixture (30 cm^3) containing ascorbic acid (8.5×10^{-4} mol) and PVP (5.0×10^{-3} mol; PVP/Pd molar ratio=10). The mixture was kept under stirring at 90 °C for 3 h, and a solution of Pd NPs was obtained. The Pd NPs were cleaned up from the excess of PVP via flocculation with acetone (1/3 v/v solution/acetone), rinsed thoroughly with acetone, and redispersed in water attaining ca. 0.4 wt% Pd in the final solution.

General procedure for the catalytic reactions: For the cycloaddition reactions of CO_2, isocyanide and 2-iodoanilines, a typical step is as follows. First, 2-iodoaniline (0.3 mmol), tert-butyl isocyanide (0.45 mmol), and 1,8-diazabicyclo[5.4.0]undec-7-ene (DBU) (0.6 mmol) were added in 2 mL of anhydrous MeCN in a 25 mL Schlenk tube. After all substrates were dissolved, the catalyst was added, and the catalytic reaction was then carried out under a CO_2 balloon atmosphere at 80 °C for 12 h. After removing the COF catalyst by centrifugation, the filtrate was extracted with ethyl acetate and was

then concentrated under vacuum to obtain the crude product, which was further purified by silica gel chromatography with the mixture of ethyl acetate/petroleum ether as the eluent. The yield of product was quantified by ^{1}H NMR analyses.

The Recycling experiment of Pd@TA-OCH_3

After reaction, the catalyst was firstly collected by centrifugation. Then, it was washed stepwise with CH_2Cl_2 (3 × 5 ml), distilled water (3 × 5 ml) and ethanol (3 × 5 ml). At last, the catalyst was dried under vacuum at 60 ^{o}C overnight and be directly used for the next catalytic run.

2. Results and Discussion

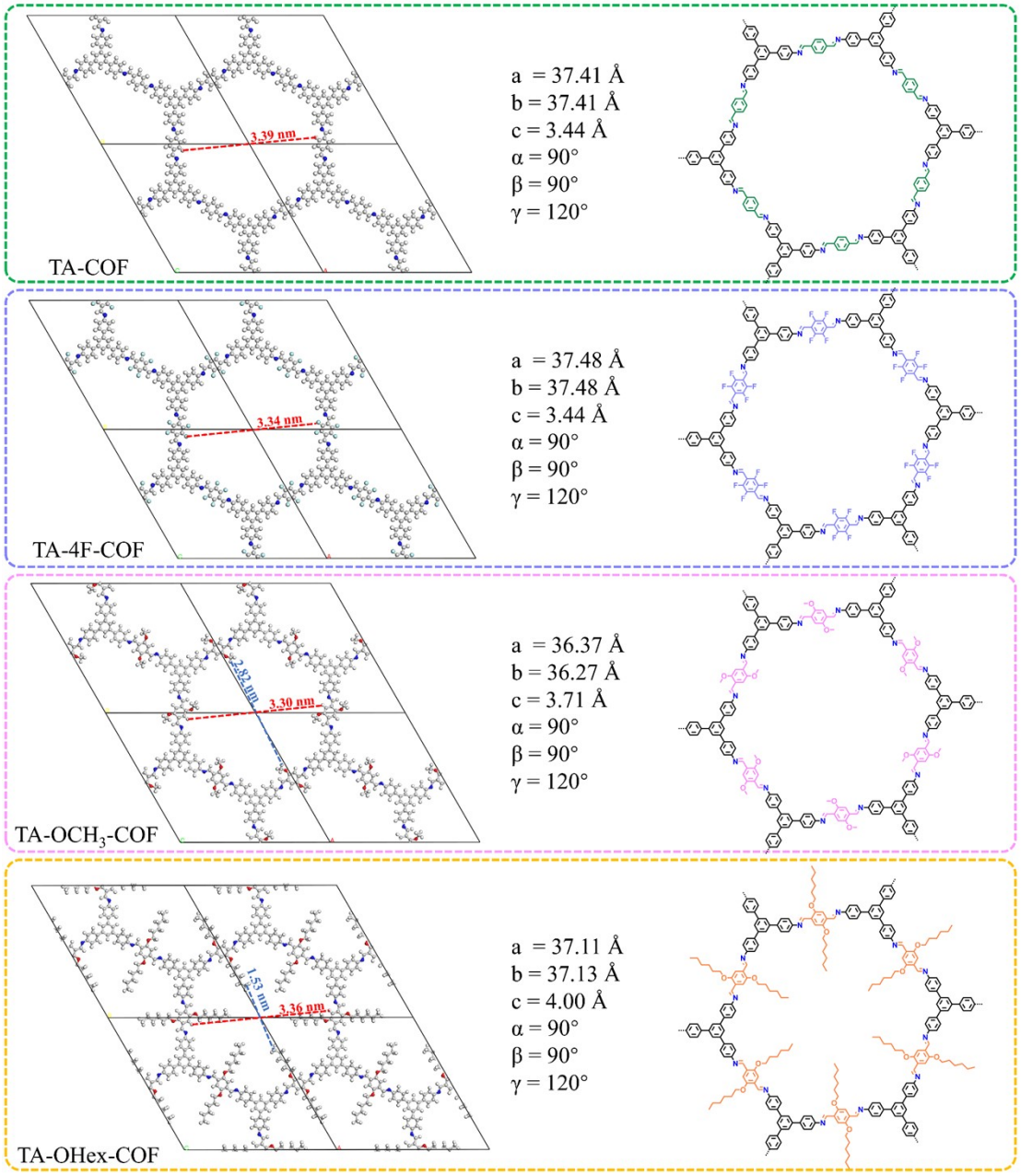

Figure S1. The chemical structure simulation and molecular formula illustration of COF-TA, TA-4F, TA-OCH_3, TA-OHex.

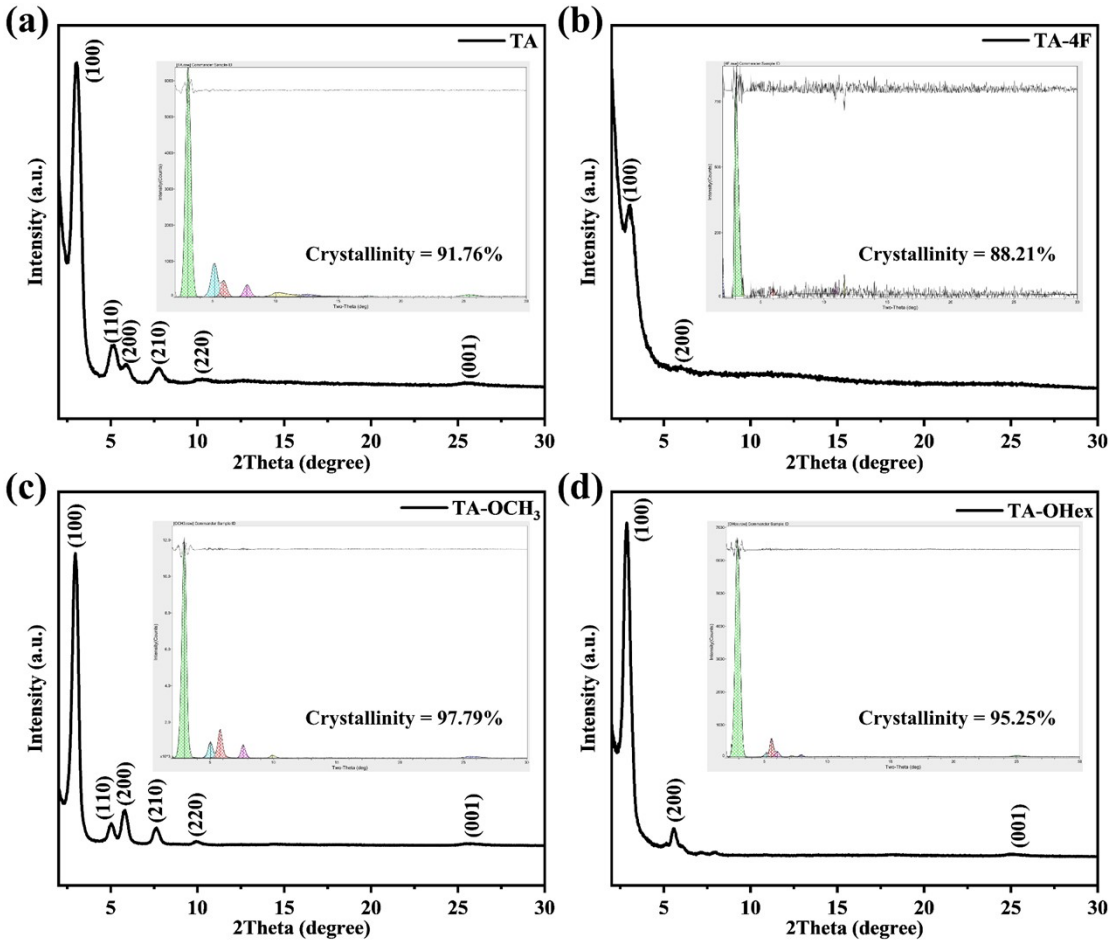

Figure S2. PXRD patterns and crystallinity index of (a) TA, (b) TA-4F, (c) TA-OCH_3, (d) TA-OHex.

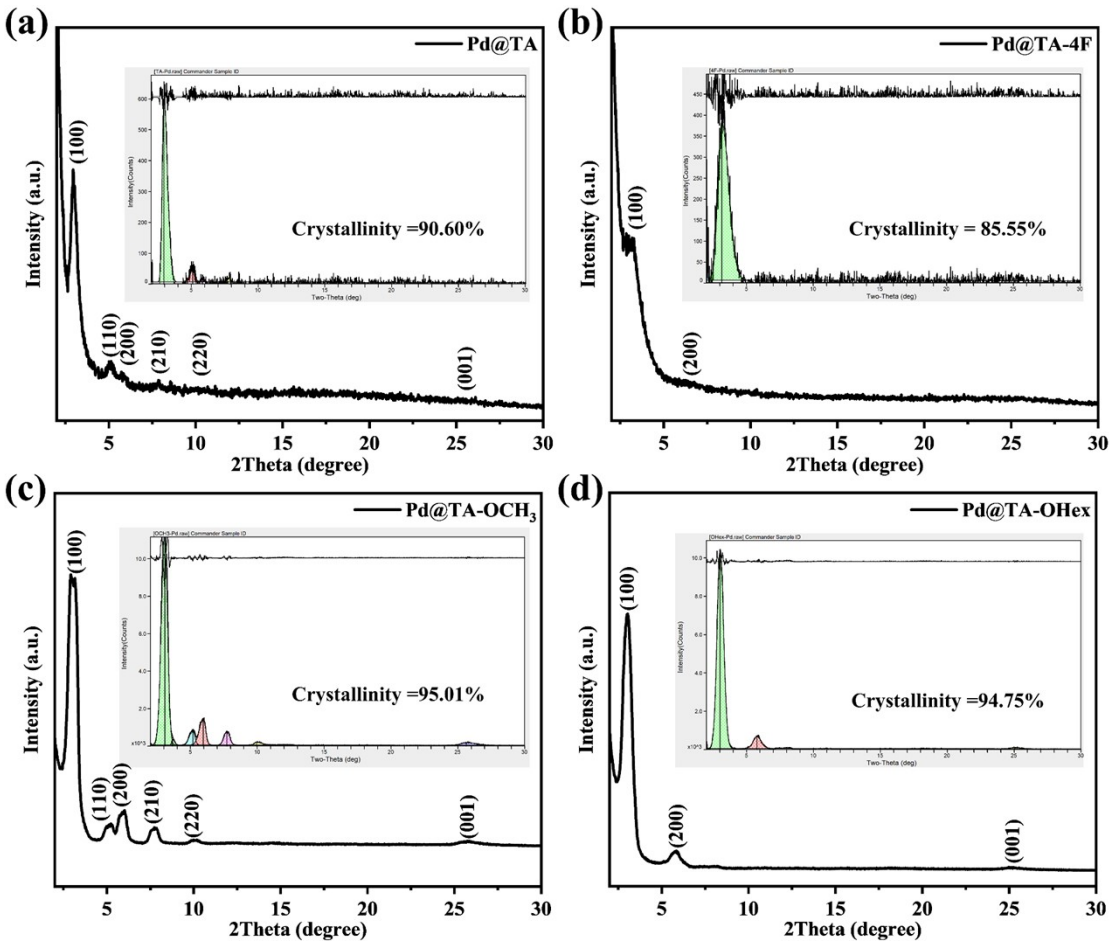

Figure S3. PXRD patterns and crystallinity index of (a) Pd@TA, (b) Pd@TA-4F, (c) Pd@TA-OCH_3, (d) Pd@TA-OHex.

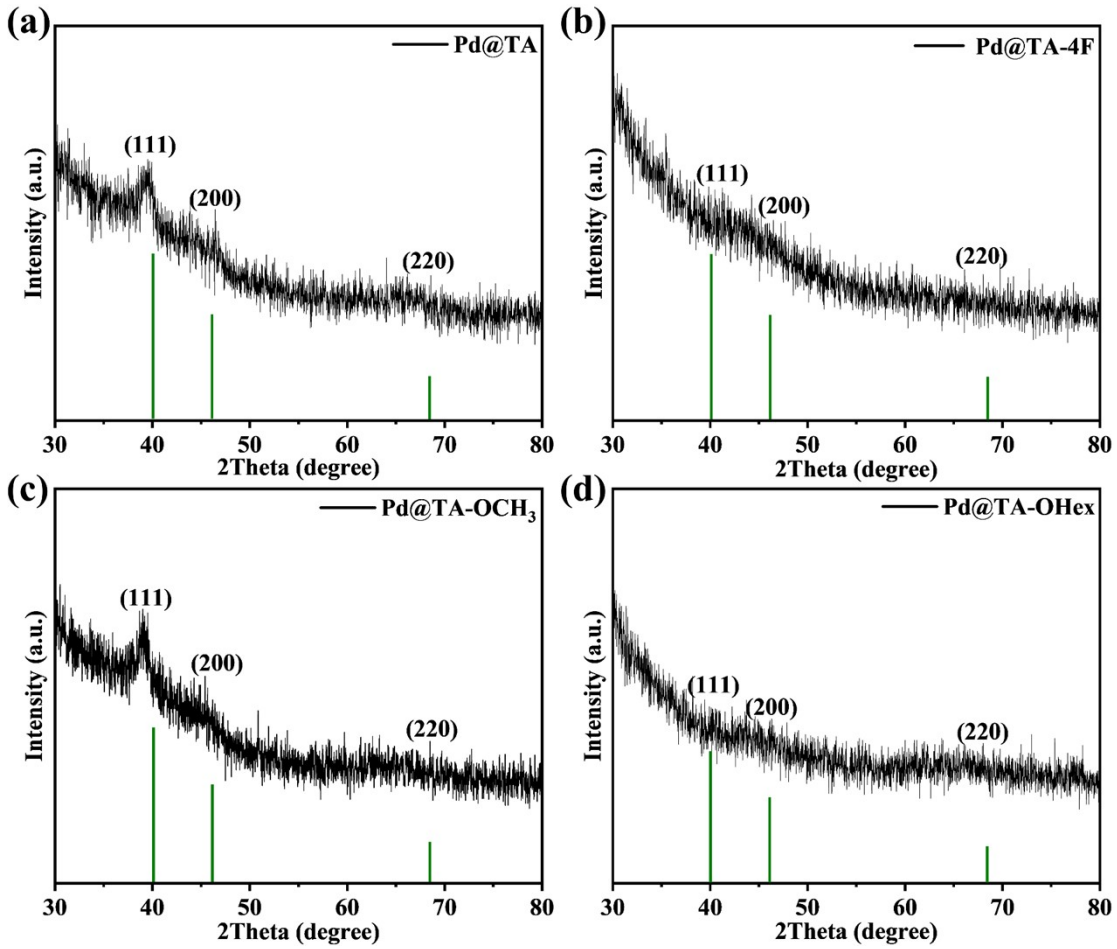

Figure S4. PXRD patterns of (a) Pd@TA, (b) Pd@TA-4F, (c) Pd@TA-OCH_3, (d) Pd@TA-OHex.

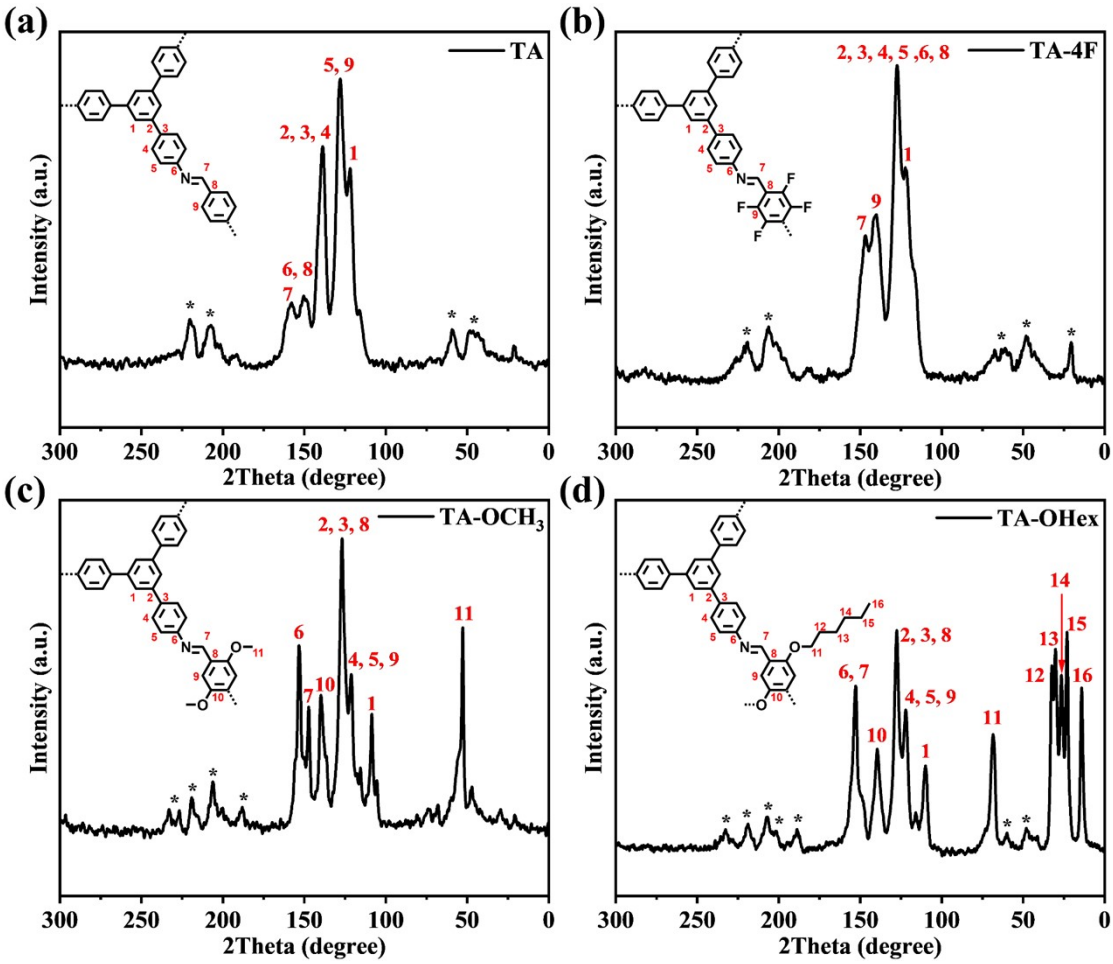

Figure S5. ^{13}C CP-MAS NMR spectra of a) TA, b) TA-4F, c) TA-OCH_3 and d) TA-OHex.

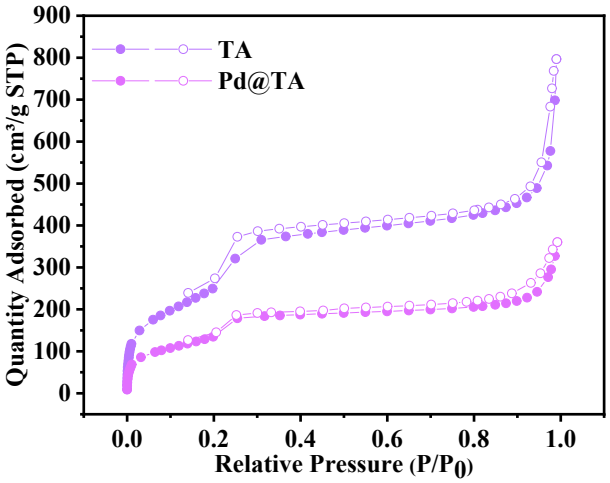

Figure S6. N_2 adsorption and desorption isotherms of COF-TA and Pd@TA at 77 K.

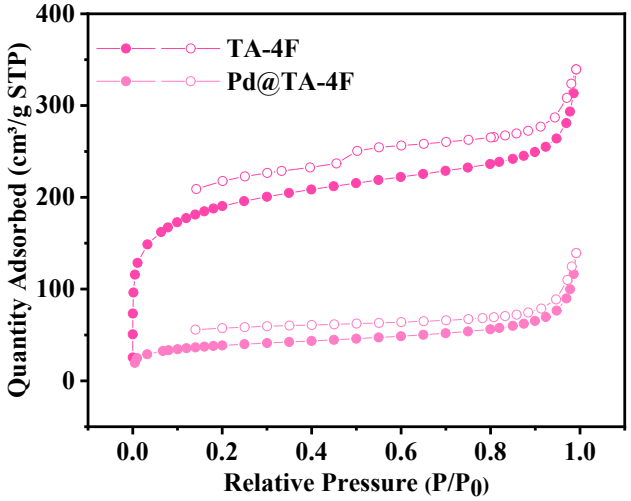

Figure S7. N_2 adsorption and desorption isotherms of COF-TA-4F and Pd@TA-4F at 77 K.

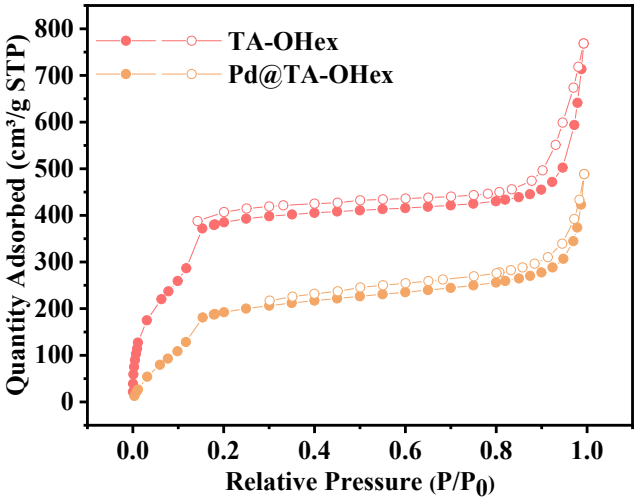

Figure S8. N_2 adsorption and desorption isotherms of COF-TA-OHex and Pd@TA-OHex at 77 K.

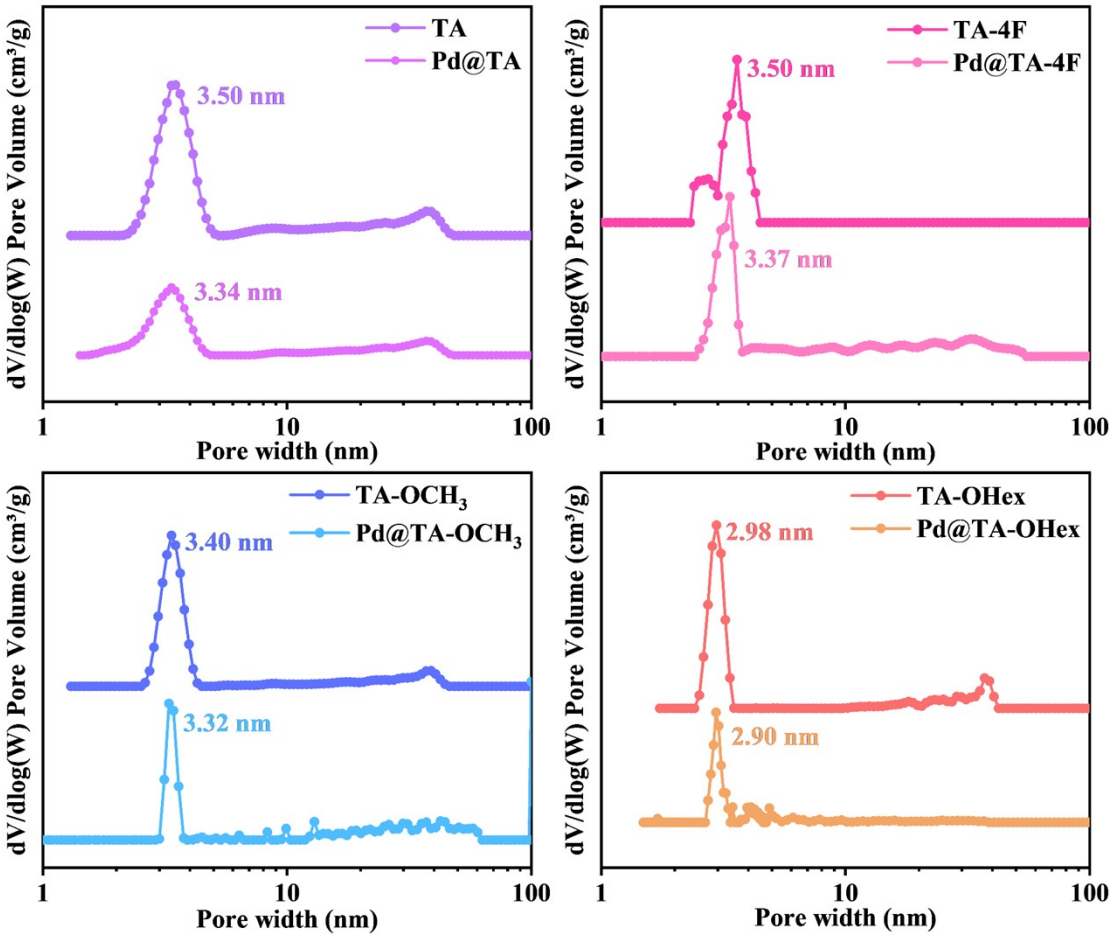

Figure S9. Pore size distribution.

Table S1. BET surface area and pore volume.

COFs	BET surface area (m^2/g)	Pore Volume (cm^3/g)	Pd@COFs	BET surface area (m^2/g)	Pore Volume (cm^3/g)
TA	1043	1.23	Pd@TA	542	0.56
TA-4F	607	0.53	Pd@TA-4F	142	0.22
TA-OCH_3	1994	2.32	Pd@TA-OCH_3	1777	1.85
TA-OHex	1535	1.19	Pd@TA-OHex	1103	0.76

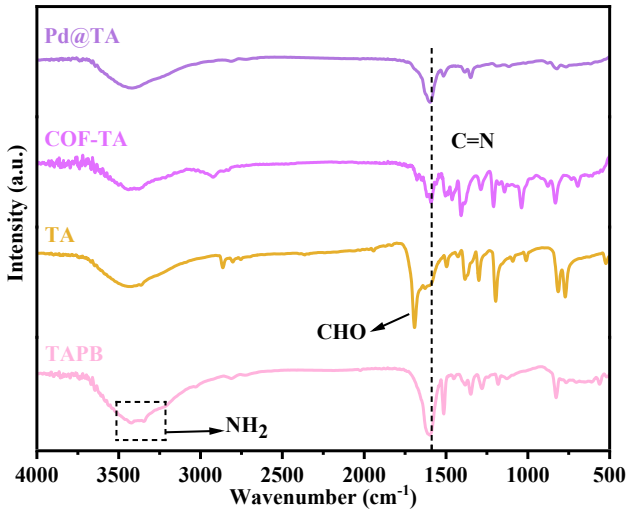

Figure S10. FT-IR spectra of TAPB, TA, COF-TA and Pd@TA.

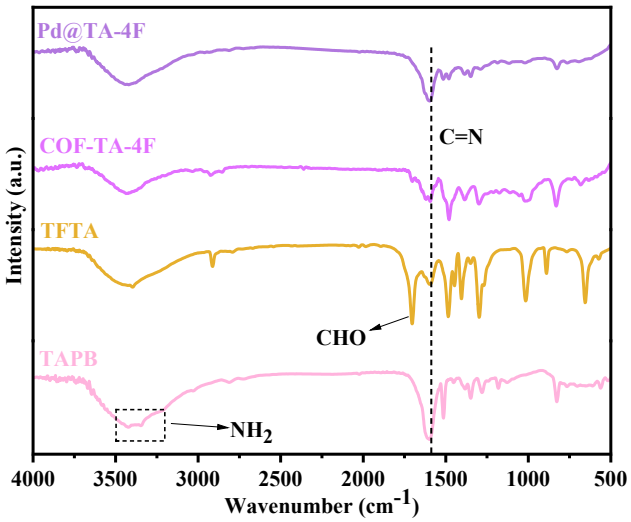

Figure S11. FT-IR spectra of TAPB, TA, COF-TA-4F and Pd@TA-4F.

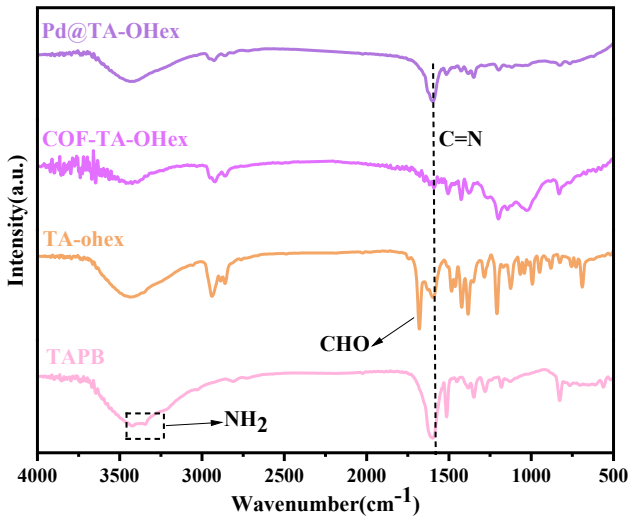

Figure S12. FT-IR spectra of TAPB, TA, COF-TA-OHex and Pd@TA-OHex.

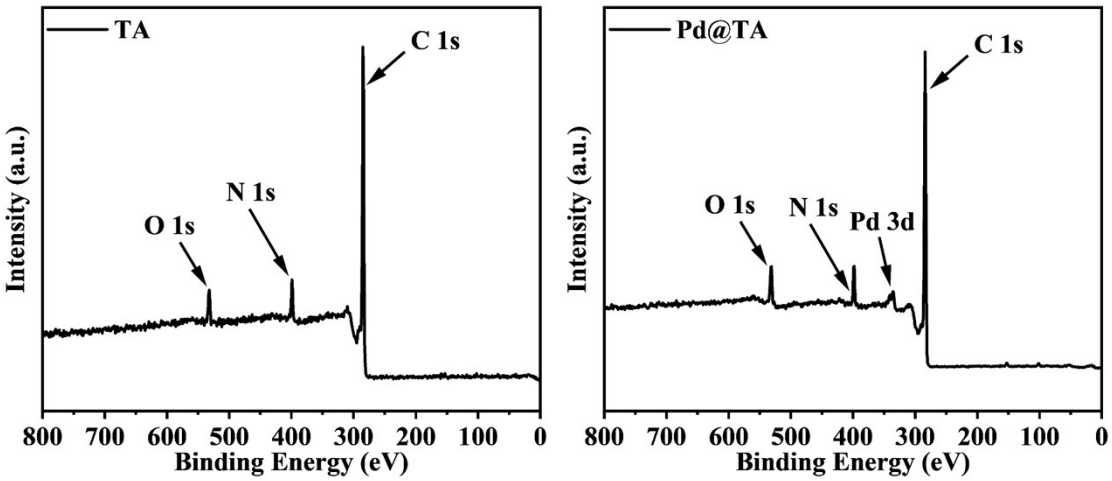

Figure S13. XPS survey of COF-TA and Pd@TA.

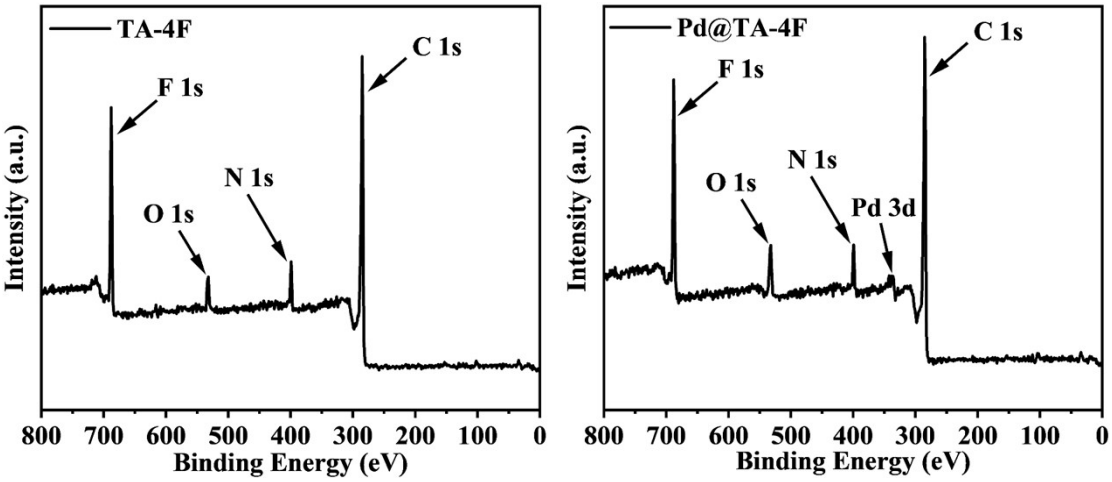

Figure S14. XPS survey of COF-TA-4F and Pd@TA-4F.

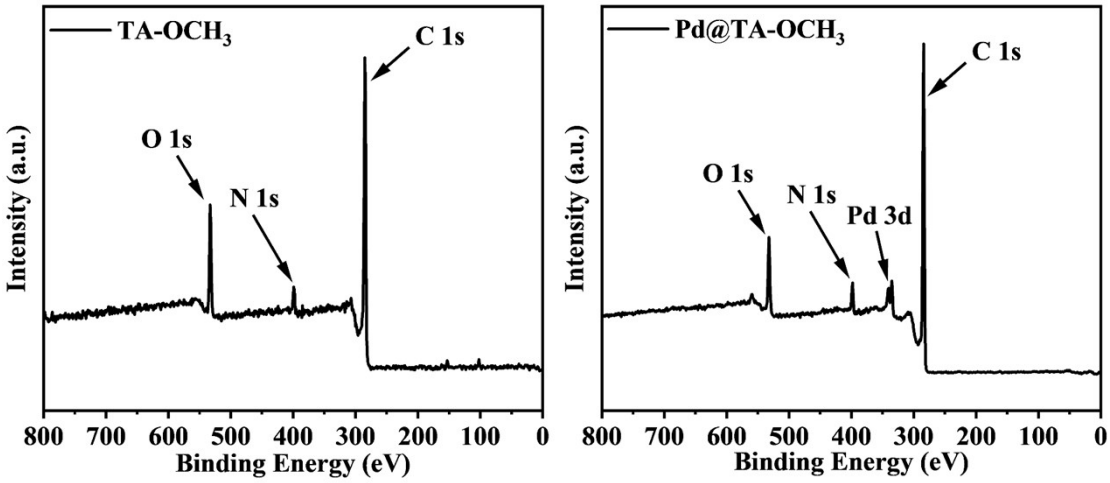

Figure S15. XPS survey of COF-TA-OCH_3 and Pd@TA-OCH_3.

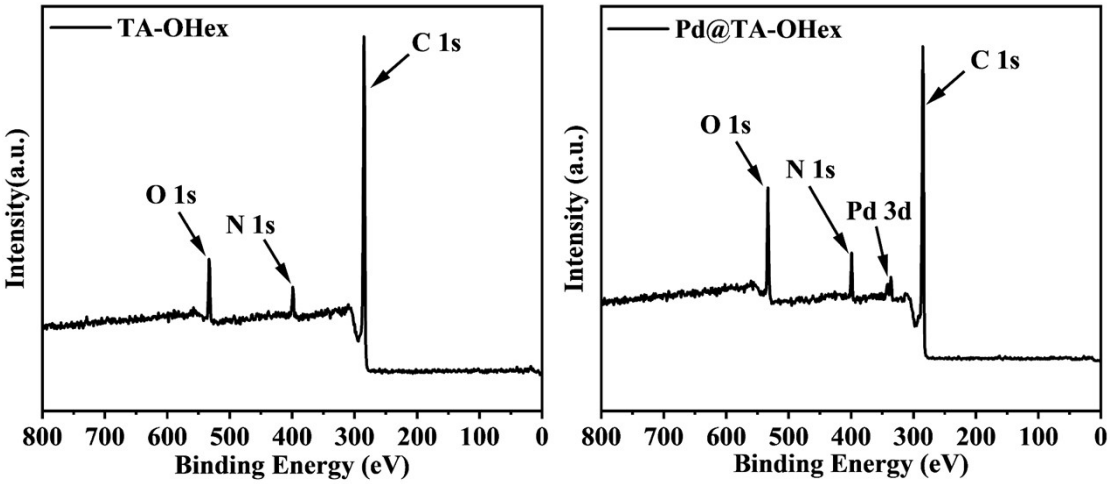

Figure S16. XPS survey of COF-TA-OHex and Pd@TA-OHex.

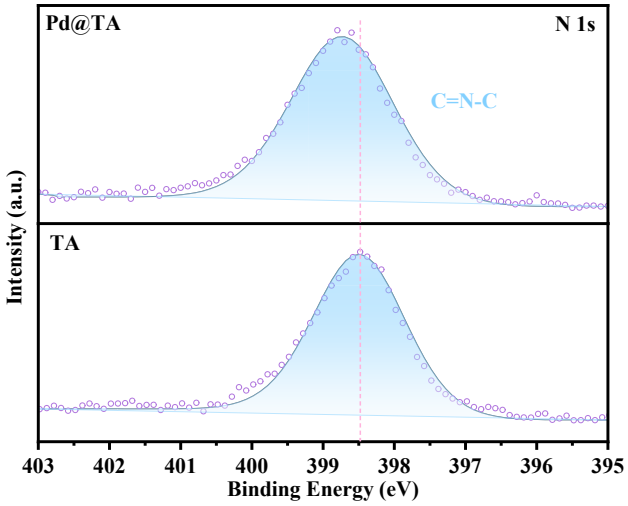

Figure S17. XPS spectra in N 1s region of COF-TA and Pd@TA.

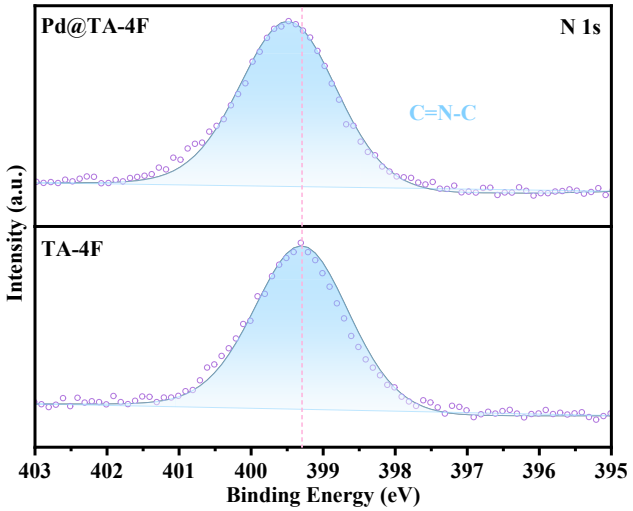

Figure S18. XPS spectra in N 1s region of COF-TA-4F and Pd@TA-4F.

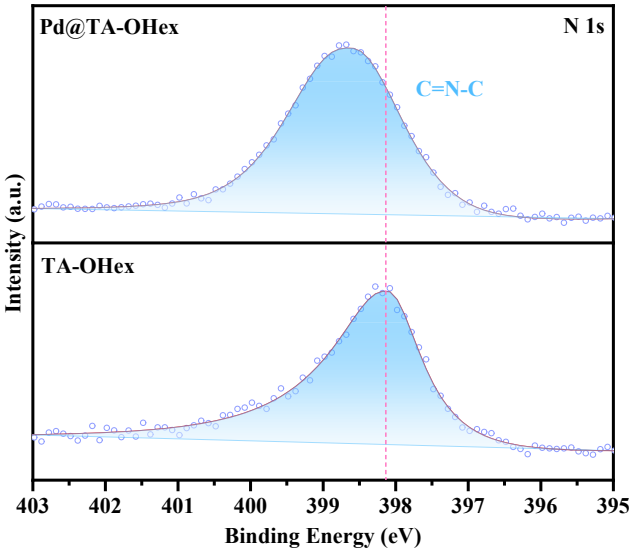

Figure S19. XPS spectra in N 1s region of COF-TA-OHex and Pd@TA-OHex.

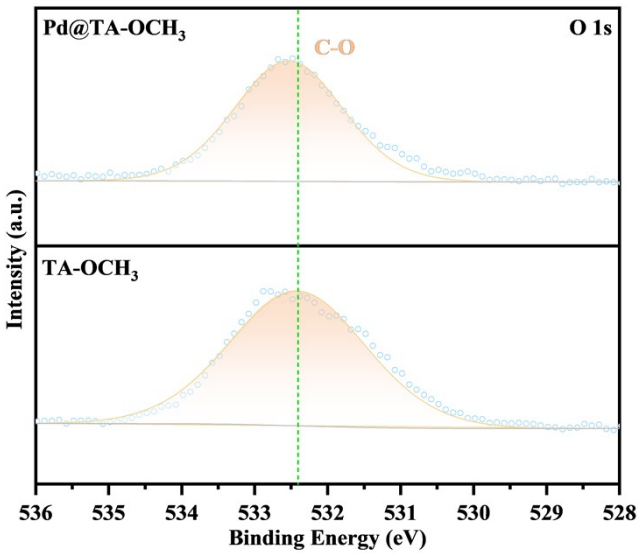

Figure S20. XPS spectra in N 1s region of COF-TA-OCH_3 and Pd@TA-OCH_3.

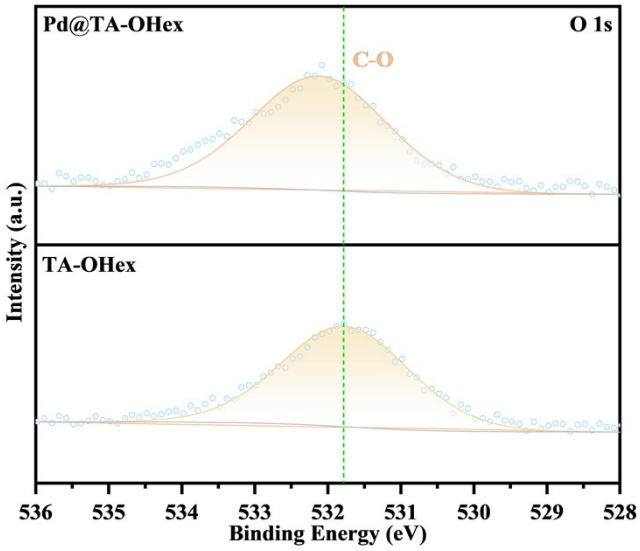

Figure S21. XPS spectra in N 1s region of COF-TA-OHex and Pd@TA-OHex.

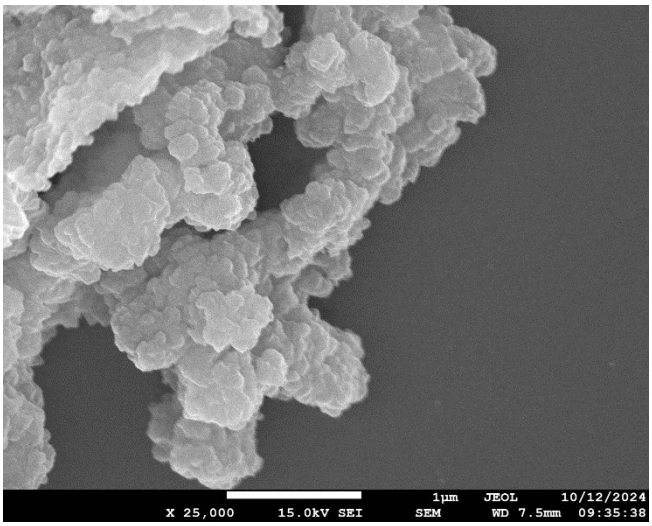

Figure S22. SEM image of COF-TA.

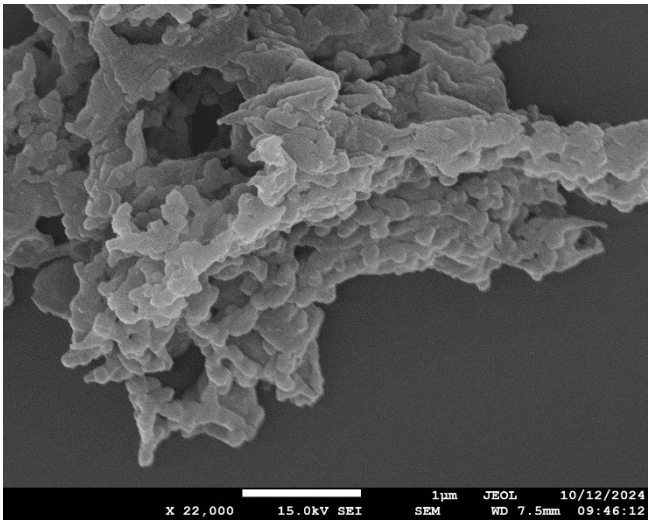

Figure S23. SEM image of COF-TA-4F.

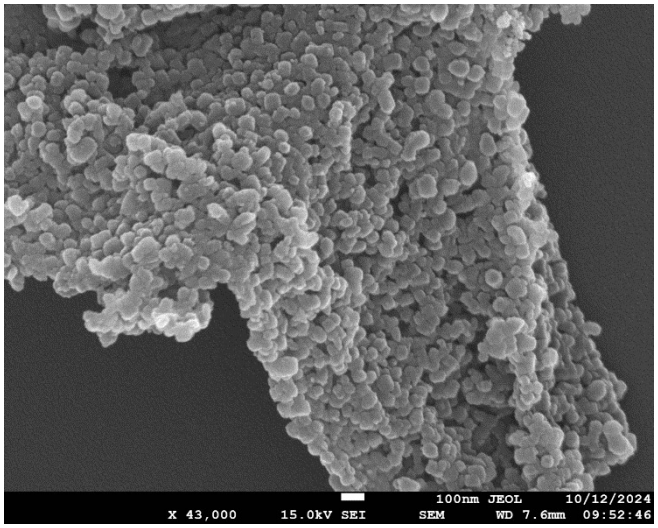

Figure S24. SEM image of COF-TA-OCH_3.

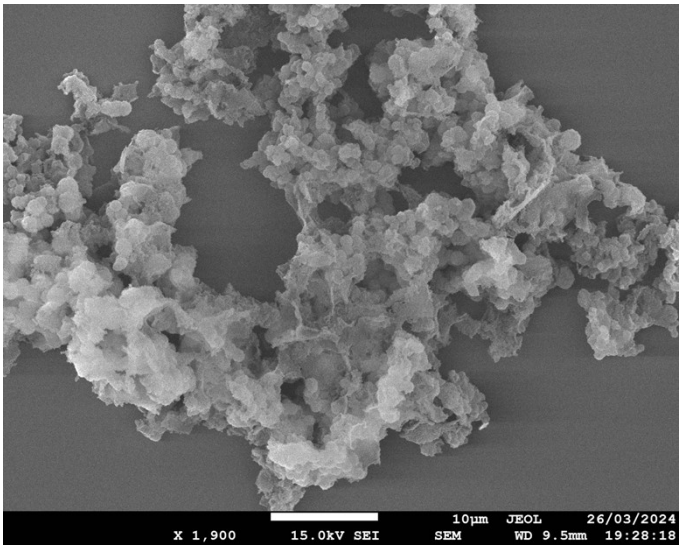

Figure S25. SEM image of COF-TA-OHex

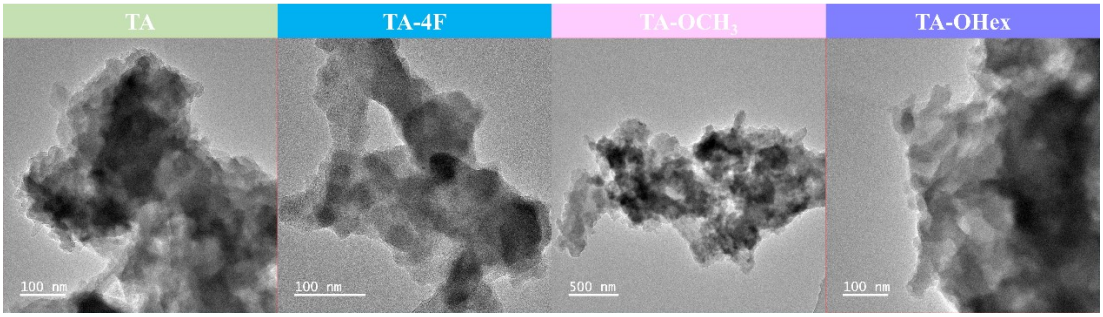

Figure S26. TEM images of COF-TA, TA-4F, TA-OCH_3 and TA-OHex.

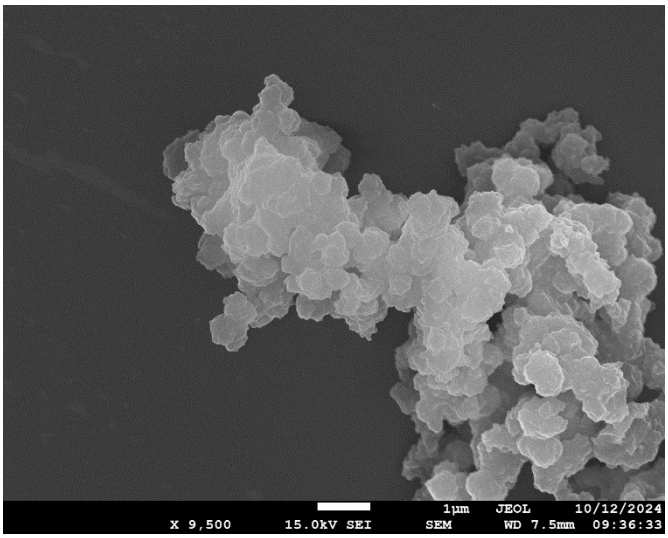

Figure S27. SEM image of Pd@TA

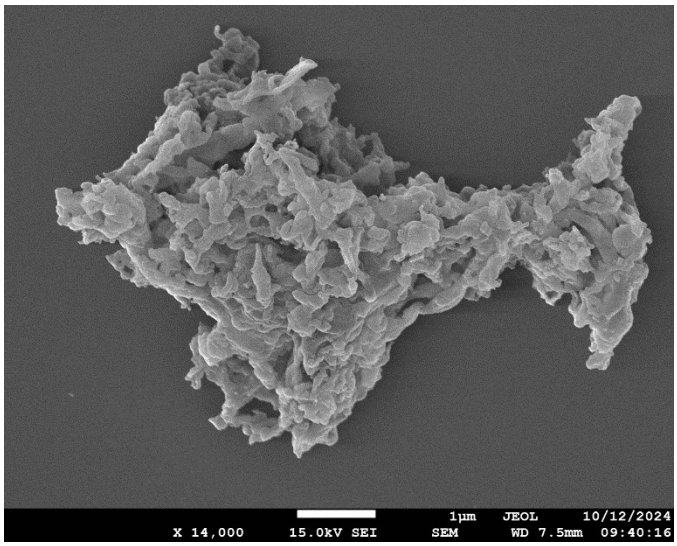

Figure S28. SEM image of Pd@TA-4F

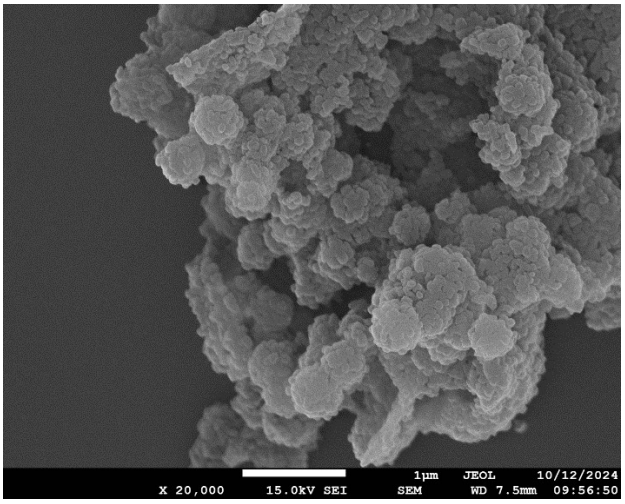

Figure S29. SEM image of Pd@TA-OCH_3.

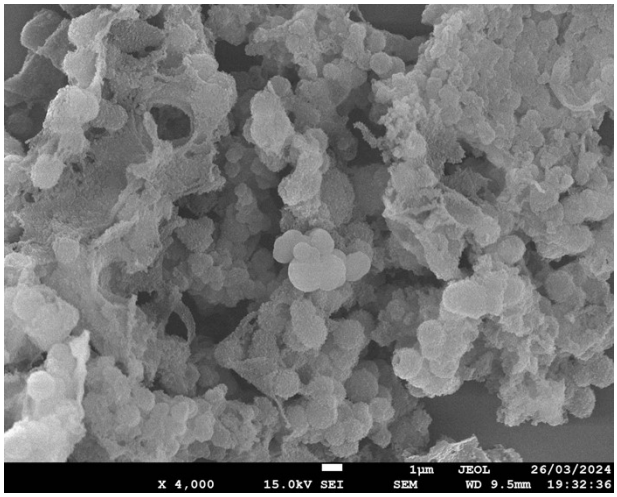

Figure S30. SEM image of Pd@TA-OHex.

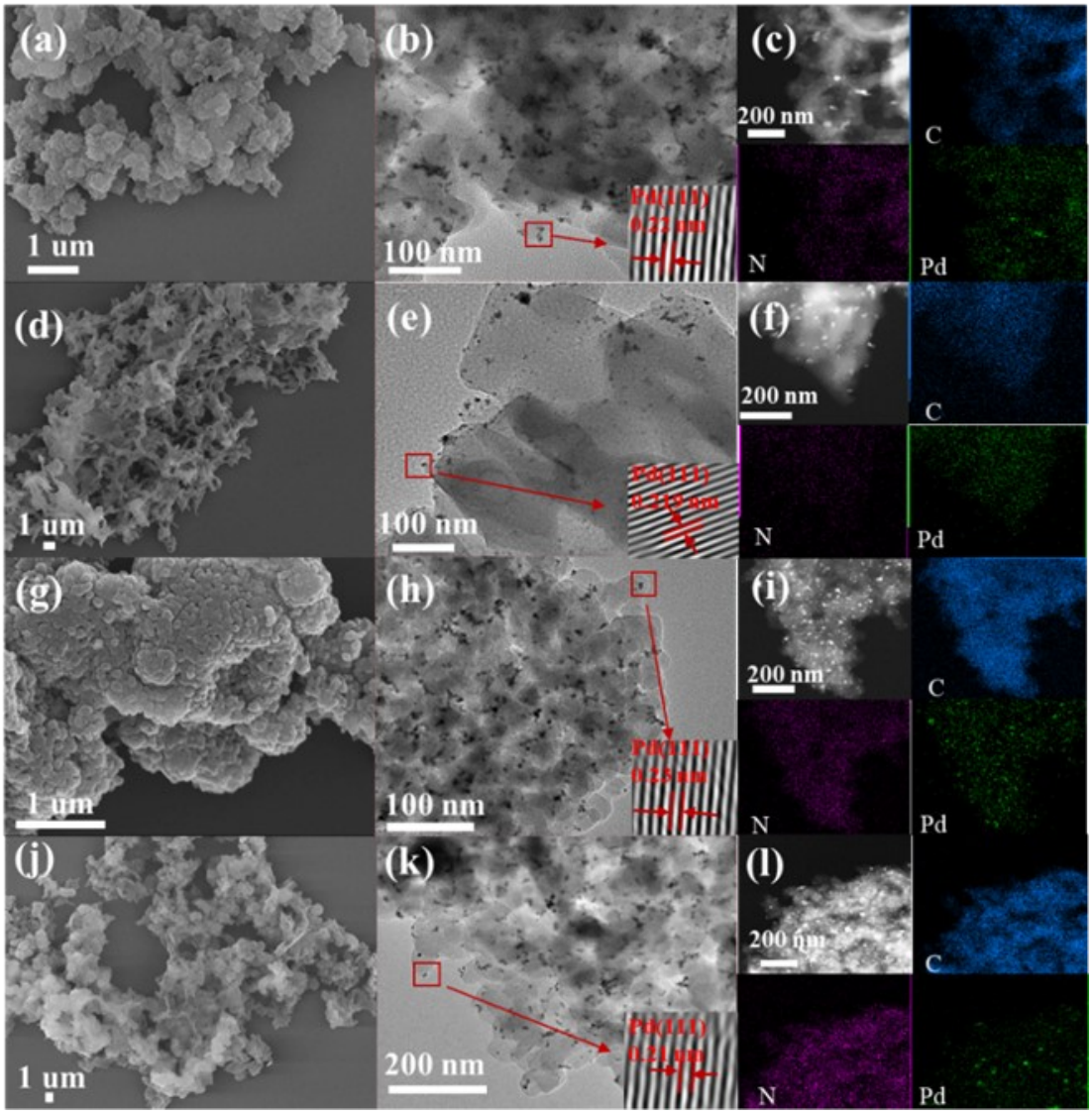

Figure S31. Scanning electron microscopy images of (a) Pd@TA; (d) Pd@TA-4F; (g) Pd@TA-OCH_3; (j) Pd@TA-OHex; transmission electron microscopy images and high-resolution images of palladium nanoparticles (b) Pd@TA; (e) Pd@TA-4F; (h) Pd@TA-OCH_3; (k) Pd@TA-OHex; EDS spectra (c) Pd@TA; (f) Pd@TA-4F; (i) Pd@TA-OCH_3; (l) Pd@TA-OHex.

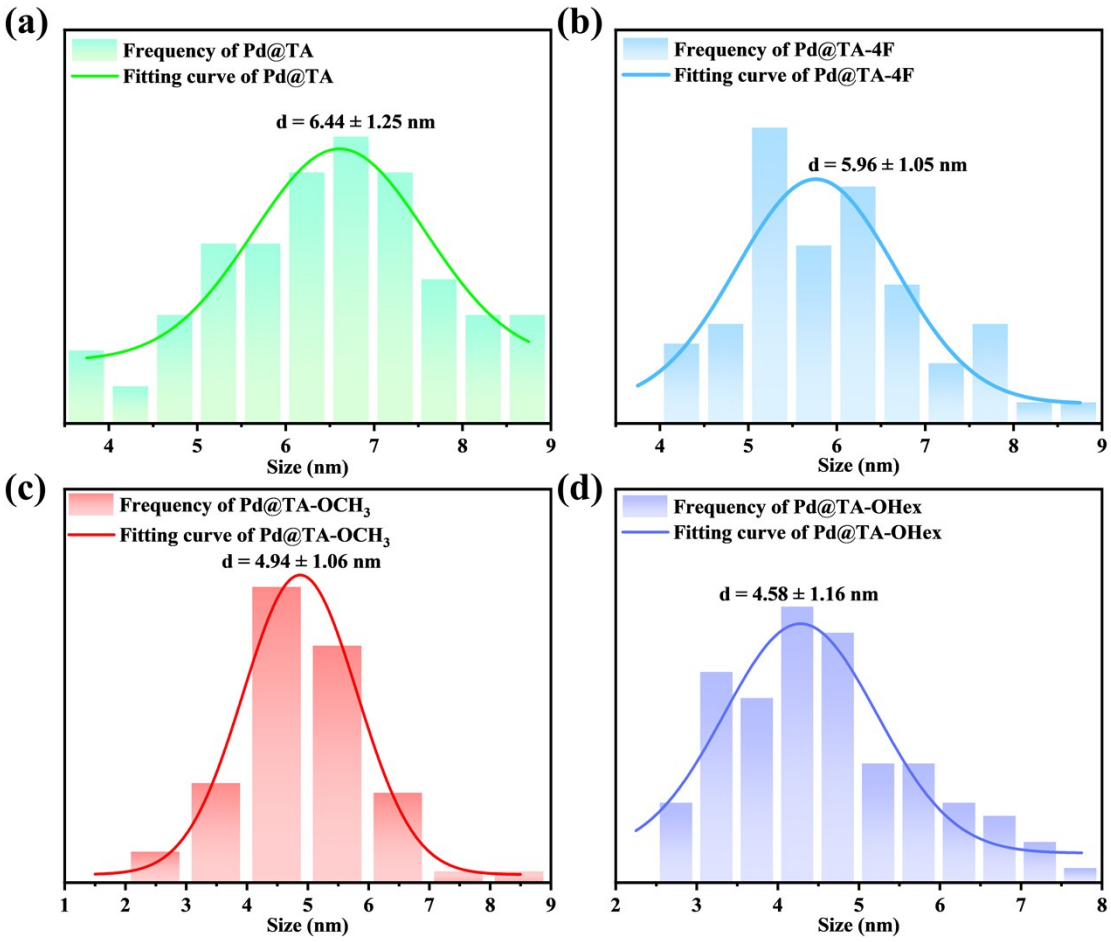

Figure S32. The particle size distribution of Pd NPs

Table S2. Optimization of catalytic conditions

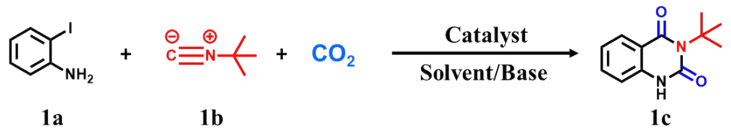

1a 1b 1c

Entry	Variation from the standard conditions[a]	Yield/%
1	**None**	**98**
2	9 h/18 h	90/99
3	60 ℃	81
4	CS_2CO_3 instead of DBU	78
5	DMSO/DMF/1,4-dioxane instead of MeCN	88/54/75
6	Pd@TA instead of Pd@TA-OCH_3	64
7	Pd@TA-4F instead of Pd@TA-OCH_3	55
8	Pd@TA-OHex instead of Pd@TA-OCH_3	70
9	Pd@Pd$(OAc)_2$ instead of Pd@TA-OCH_3	82
10	A physical mixture of Pd$(OAc)_2$ and TA-OCH_3	27
11	TA-OCH_3 instead of Pd@TA-OCH_3	trace
12	Pd NPs instead of Pd@TA-OCH_3	41
13	A physical mixture of Pd NPs and TA-OCH_3	34

[a]Standard condition: 2-iodoaniline (0.3 mmol), tert-butyl isocyanide (0.45 mmol), and 1,8-diazabicyclo[5.4.0]undec-7-ene (DBU) (0.6 mmol), Pd@TA-OCH_3 (5 mg), MeCN (2 mL), CO_2 balloon, 80 ℃, 12 h.

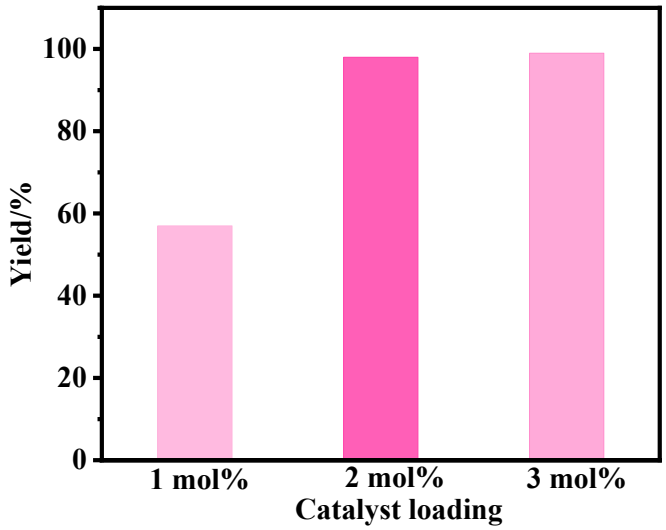

Figure S33. Effect of the catalyst loading on yield.

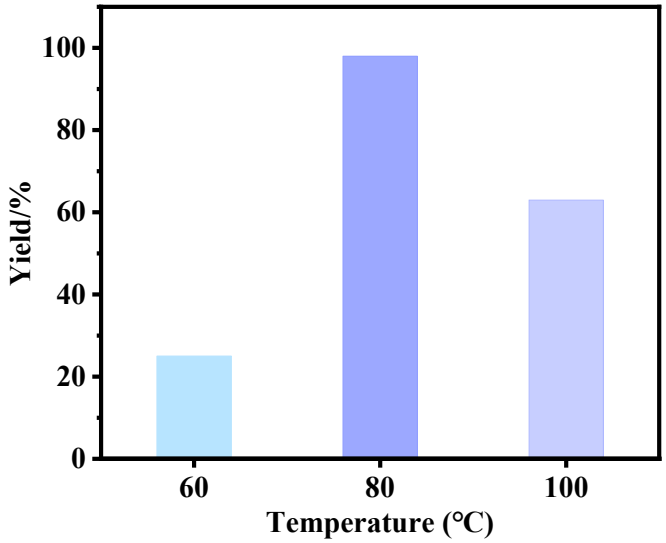

Figure S34. Effect of the reaction temperature on yield.

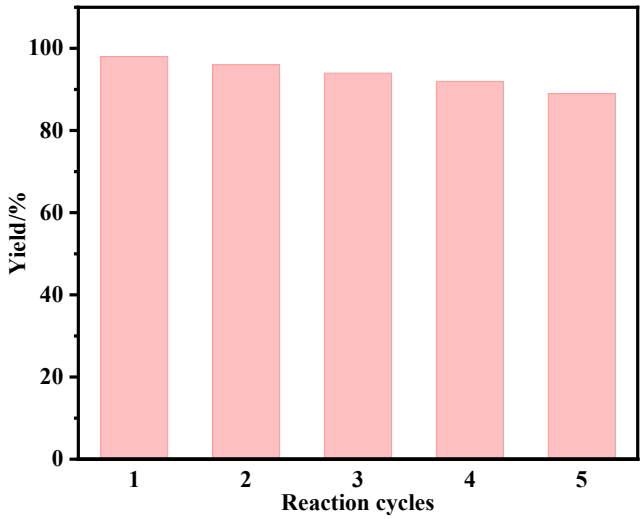

Figure S35. Cyclic performance test.

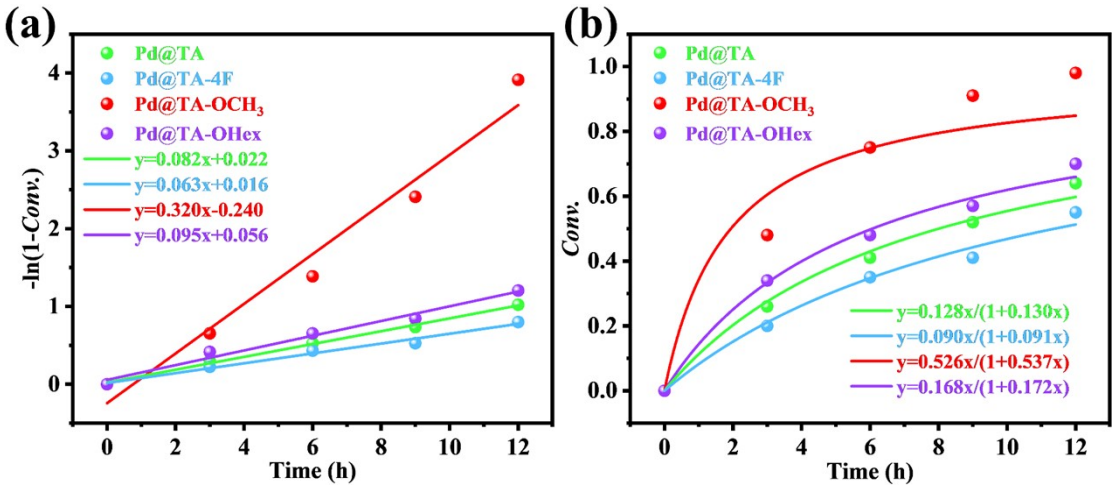

Figure S36. (a) First-order and (b) Second-order kinetics study of the reaction.

Table S3. Kinetic fitting parameters.

First-order kinetics	Equation	Rate Constant (k)	Correlation Coefficient (R^2)	Average value
Pd@TA	y=0.082x+0.022	0.063 h^{-1}	0.996	0.983
Pd@TA-4F	y=0.063x+0.016	0.082 h^{-1}	0.983	
Pd@TA-OCH_3	y=0.320x-0.240	0.320 h^{-1}	0.968	
Pd@TA-OHex	y=0.095x+0.056	0.095 h^{-1}	0.985	
Second-order kinetics	**Equation**	**Rate Constant (k)**	**Correlation Coefficient (R^2)**	**Average value**
Pd@TA	y=0.128x/(1+0.130x)	0.133 h^{-1}	0.990	0.975
Pd@TA-4F	y=0.090x/(1+0.091x)	0.093 h^{-1}	0.986	
Pd@TA-OCH_3	y=0.526x/(1+0.537x)	0.548 h^{-1}	0.933	
Pd@TA-OHex	y=0.168x/(1+0.172x)	0.175 h^{-1}	0.991	

First-order kinetic equation:

$$-\ln(1-Conv.) = k_1 t \#(1)$$

Among them, $Conv.$ refers to the reaction conversion rate. NMR analysis revealed that there is only the main product, with other by-products being negligible. Therefore, the yield is used to represent the conversion rate. k_1 is the reaction rate constant, and t is the reaction time.

Second-order kinetic equation:

$$Conv. = \frac{k_2 Conv._e^2 t}{1 + k_2 Conv._e} \#(2)$$

Among them, $Conv.$ refers to the reaction conversion rate. $Conv._e$ denotes the equilibrium conversion rate. As shown in Table S2, when the reaction time is 12 h, the yield reaches 98% (Entry 1). Extending the reaction time to 18 h results in almost no change in the yield (Entry 3). Therefore, $Conv._e$ is set to 0.98 in this case. k_2 is the

reaction rate constant, and t is the reaction time.

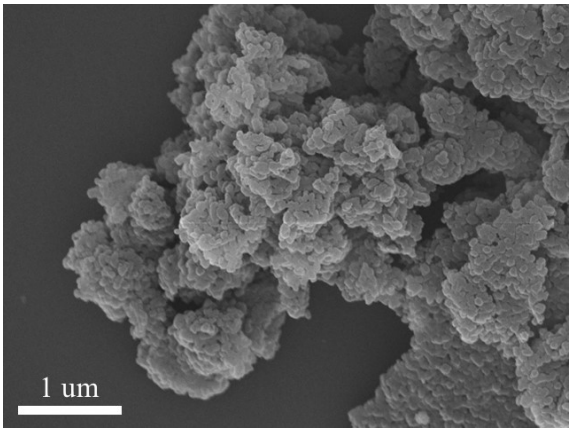

Figure S37. SEM image of Pd@TA-OCH_3 after catalysis.

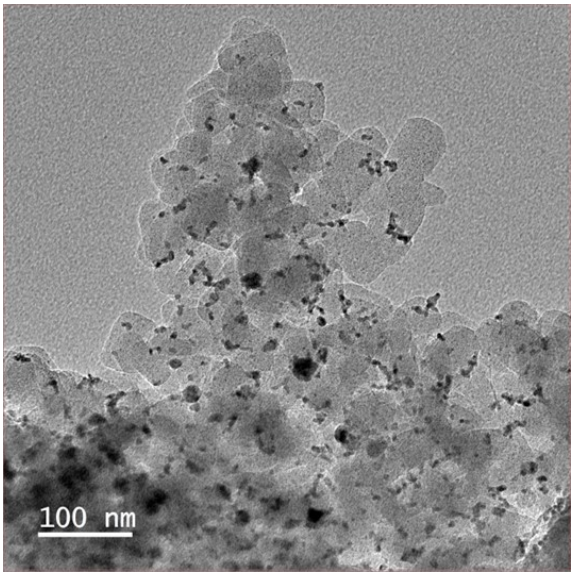

Figure S38. TEM image of Pd@TA-OCH_3 after catalysis.

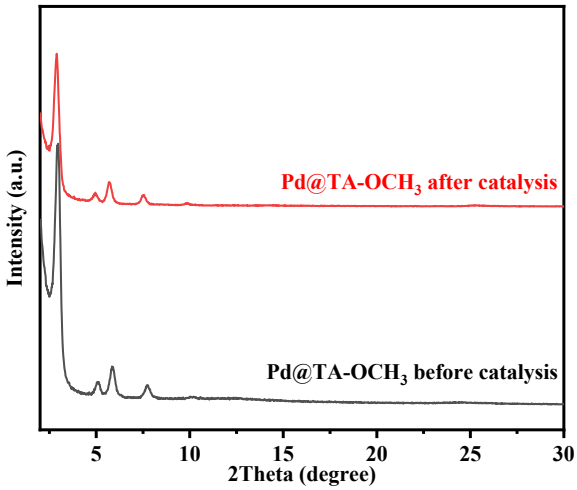

Figure S39. PXRD patterns of Pd@TA-OCH_3 after catalysis.

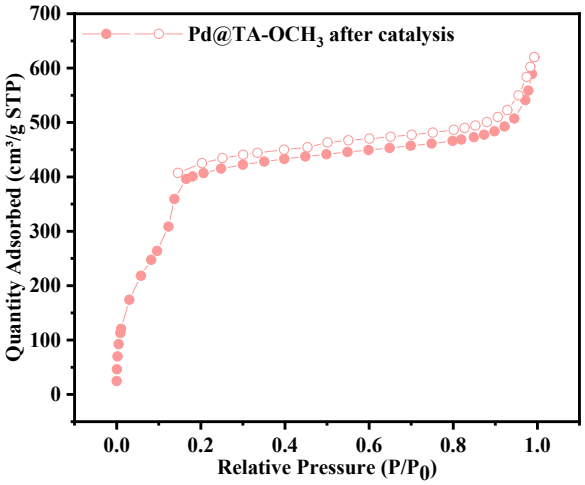

Figure S40. N_2 adsorption and desorption isotherms of Pd@TA-OCH_3 at 77 K after catalysis.

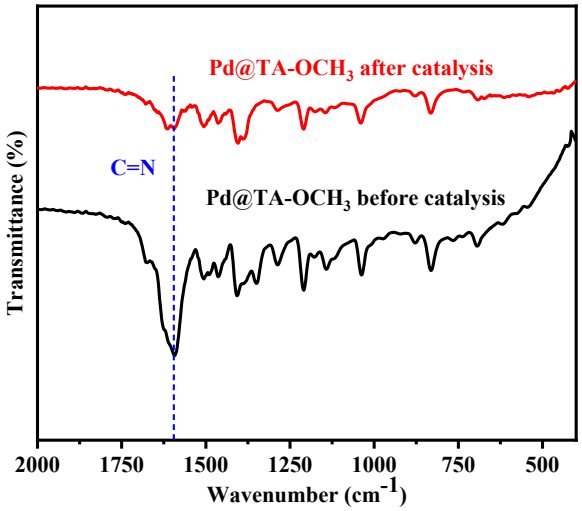

Figure S41. FT-IR spectra of Pd@TA-OCH_3 after catalysis.

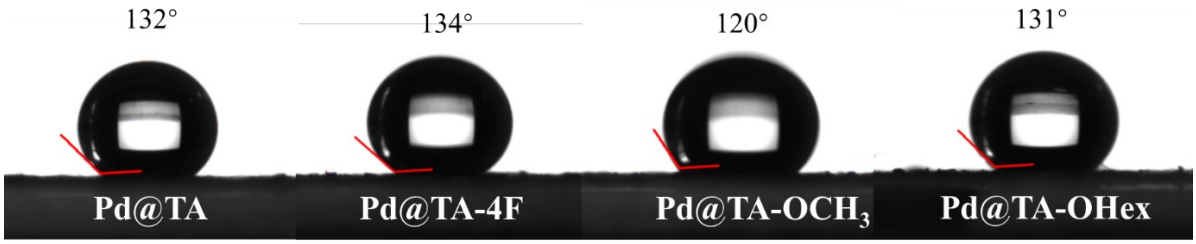

Figure S42. Water contact angel experiments of different COFs Pd catalysts.

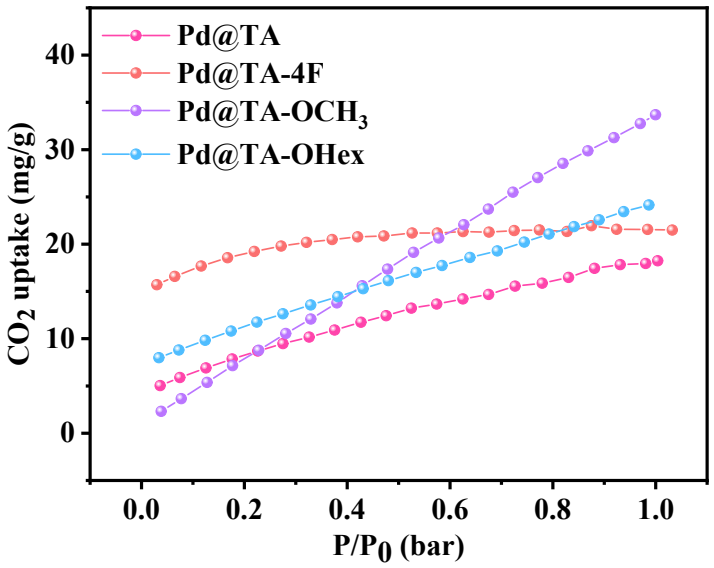

Figure S43. CO_2 adsorption isotherms for different COFs Pd catalysts at 298 K.

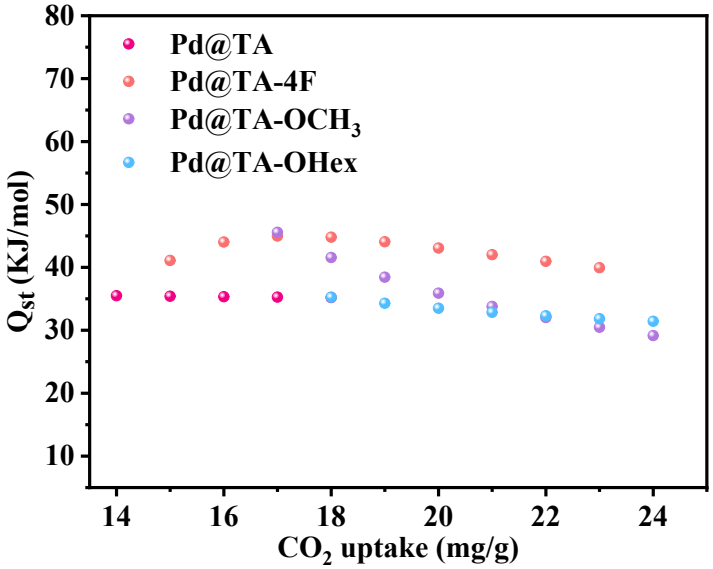

Figure S44. Enthalpy of adsorption of different COF Pd catalysts.

Table S4. Pd content in fresh Pd@TA-OCH_3 and reaction filtrate.

Catalysts	Pd content
Pd@TA-OCH_3	13.2%
Reaction filtrate	0.0052%

Table S5. Comparison of reaction conditions in different reaction systems [4-11].

Entry	Catalytic system	Ligand	Pd loading or Cat.	t (h)	T (℃)	CO_2 pressure	Base	Solvents	Yield (%)	Source
1	Pd@TA-OCH_3	No	5 mg, 2 mol%	12	80	1 atm	DBU	MeCN	98	This work
2	$Pd(OAc)_2$	$BuPAd_2$	10 mol%	7	80	10 bar	CS_2CO_3	1,4-dioxane	91	Ref.(4)
3	$Pd(CH_3CN)_2Cl$	Sphos	10 mol%	24	90	2 MPa	CS_2CO_3	DMSO	90	Ref.(5)
4	Pd(II)EN@GO	No	50 mg	10	80	1 atm	DBU	MeCN	94	Ref.(6)
5	$PdCl_2$	PPh_3	10 mol%	12	80	1 atm	DBU	MeCN	97	Ref.(7)
6	Pd(0)@POL-TBZP	No	0.02 mol%	12	90	1 atm	DBU	DMSO	95	Ref.(8)
7	Pd NCs@ZIF-8	No	11.2 wt%	10	80	1 atm	DBU	MeCN	92	Ref.(9)
8	Pd@POP-1	No	0.168 mol%	18	60	1 atm	DBU	MeCN	92	Ref.(10)
9	Pd/MIL-101-PPh_3	No	0.15 mol%	3	80	1 atm	DBU	MeCN	92	Ref.(11)

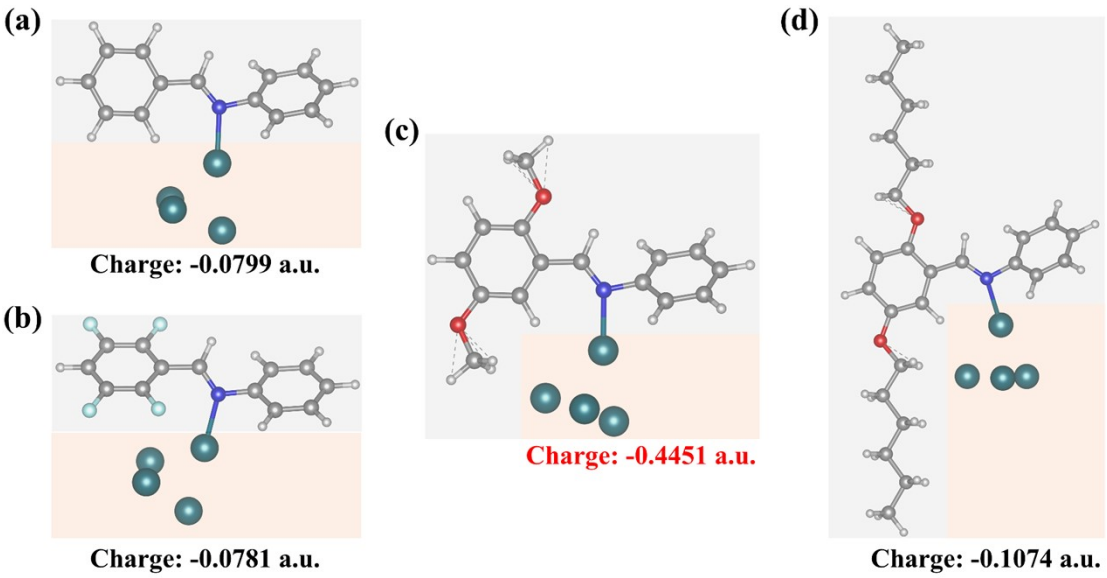

Figure S45. Calculated charge of the Pd cluster in (a) Pd@TA, (b) Pd@TA-4F, (c) Pd@TA-OCH_3, (d) Pd@TA-OHex.

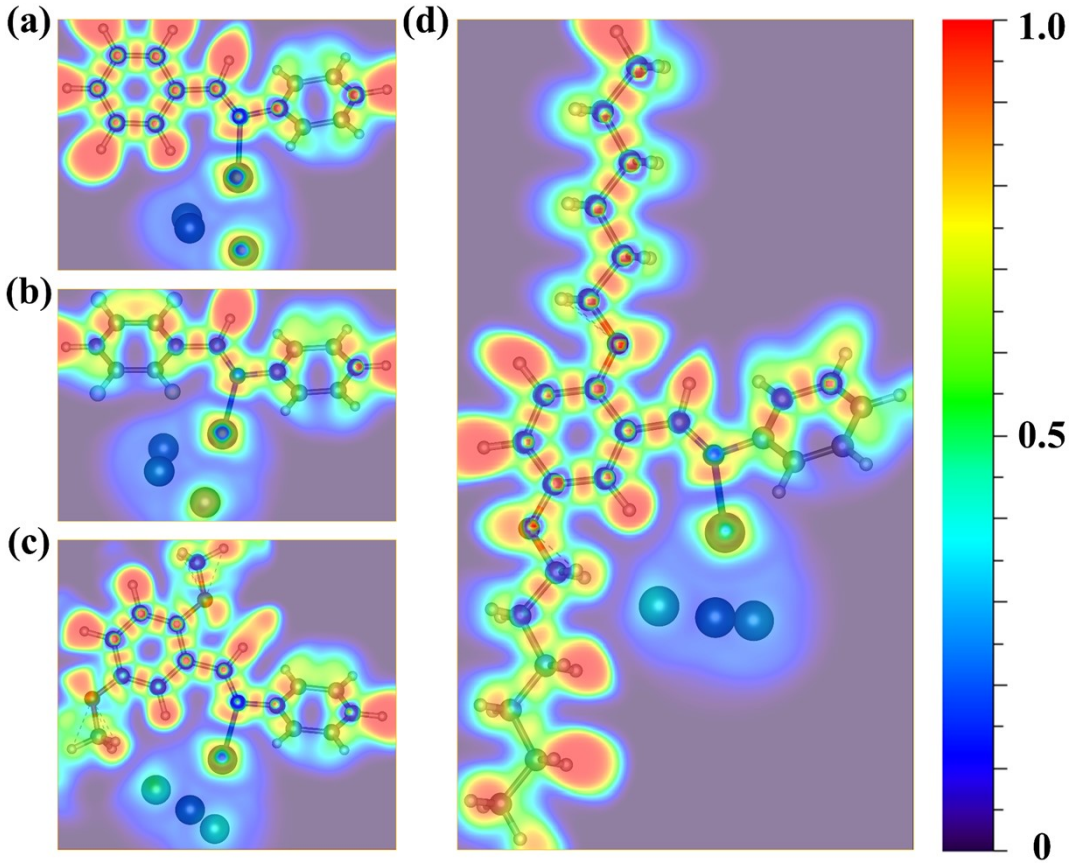

Figure S46. The calculated ELF diagrams of (a) Pd@TA, (b) Pd@TA-4F, (c) Pd@TA-OCH_3, (d) Pd@TA-OHex.

3. NMR Analysis of Oxazolidinone Products

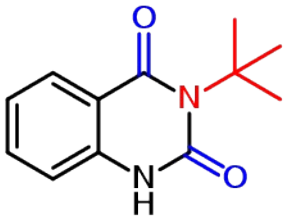

3-(tert-butyl)quinazoline-2,4(1H,3H)-dione (3a): yield: 98%. White solid. ^{1}H NMR (400 MHz, $CDCl_3$): δ = 9.87 (s, 1H), 7.95-7.93 (d, J = 7.4 Hz, 1H), 7.49-7.46 (m, 1H), 7.19-7.08 (m, 1H), 6.93 (d, J = 8.1 Hz, 1H), 1.73 (s, 9H). ^{13}C NMR (100 MHz, $CDCl_3$): δ = 163.3, 152.0, 137.0, 133.3, 127.1, 121.8, 116.0, 112.9, 61.0, 28.9.

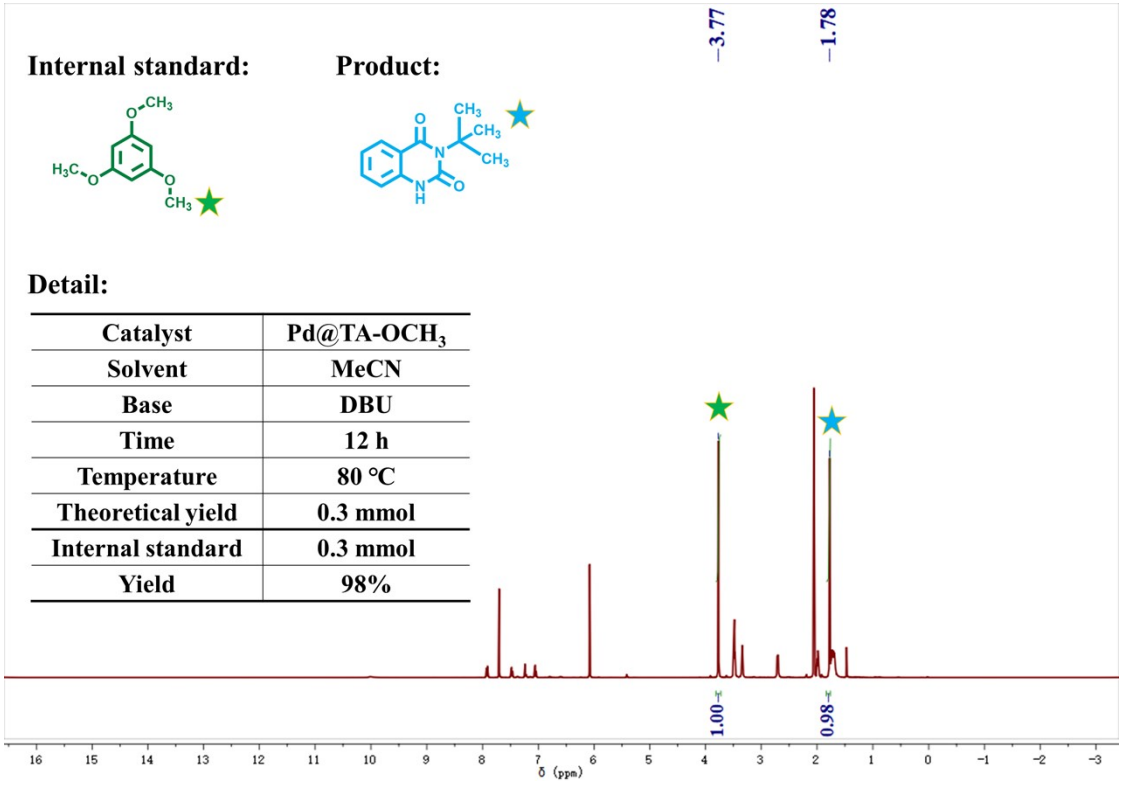

Figure S47. ^{1}H NMR determination of yield.

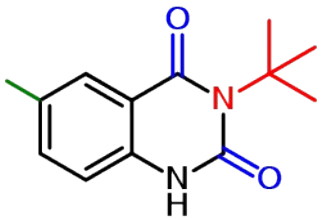

3-(tert-butyl)-6-methylquinazoline-2,4(1H,3H)-dione (3b): yield: 70%. Gray solid. ^{1}H NMR (400 MHz, $CDCl_3$): δ = 9.38 (d, J = 51.8 Hz, 1H), 7.74-7.73 (s, 1H), 7.29-7.27 (dd, J = 8.2, 1.6 Hz, 1H), 6.81 (d, J = 8.2 Hz, 1H), 2.30 (s, 3H), 1.71 (s, 9H). ^{13}C NMR (100 MHz, $CDCl_3$): δ = 163.4, 151.7, 134.7, 134.4, 131.5, 126.7, 115.8, 112.8, 60.9, 28.9, 19.8.

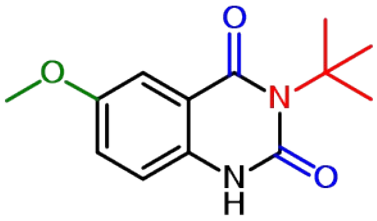

3-(tert-butyl)-6-methoxyquinazoline-2,4(1H,3H)-dione (3c): Brown solid, yield: 69%. ^{1}H NMR (400 MHz, $CDCl_3$): δ = 10.62 (s, 1H), 7.37 (s, 1H), 7.19 (dd, J = 8.8, 2.8 Hz, 1H), 7.08 (d, J = 8.7 Hz, 1H), 3.75 (s, 3H), 1.73 (s, 9H). ^{13}C NMR (100 MHz, $CDCl_3$): δ = 163.4, 154.4, 152.3, 131.4, 122.9, 116.4, 114.7, 107.6, 61.0, 54.7, 29.0.

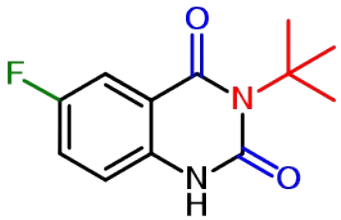

3-(tert-butyl)-6-fluoroquinazoline-2,4(1H,3H)-dione (3d): Brown solid, yield: 60%. ^{1}H NMR (400 MHz, $CDCl_3$): δ = 10.46 (s, 1H), 7.63 (d, J = 8.2 Hz, 1H), 7.20 (td, J = 8.5, 2.3 Hz, 1H), 6.94 (dd, J = 8.7, 4.1 Hz, 1H), 1.72 (s, 9H). ^{13}C NMR (100 MHz, $CDCl_3$): δ = 162.4 (J = 2.6 Hz), 158.5 (J = 241.4 Hz), 152.2, 133.5, 121.4 (J = 24.3 Hz), 117.0

(J = 8.1 Hz), 114.8 (J = 7.5 Hz), 112.7 (J = 25.7 Hz), 61.4, 28.9.

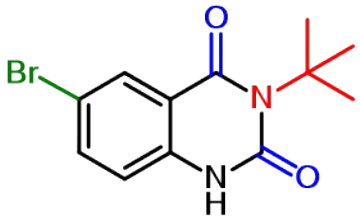

6-bromo-3-(tert-butyl)quinazoline-2,4(1H,3H)-dione (3e): Brown solid. Yield: 73%. ^{1}H NMR (400 MHz, $CDCl_3$): δ = 10.02 (s, 1H), 8.07 (d, J = 2.2 Hz, 1H), 7.56 (dd, J = 8.5, 2.2 Hz, 1H), 6.83 (d, J = 8.5 Hz, 1H), 1.70 (s, 9H). ^{13}C NMR (100 MHz, $CDCl_3$): δ = 162.0, 151.8, 136.2, 135.9, 129.7, 117.5, 114.8, 114.4, 61.5, 28.8.

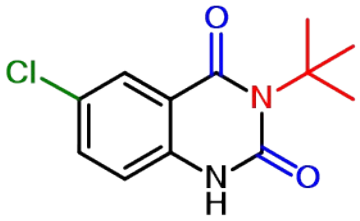

3-(tert-butyl)-6- chloroquinazoline -2,4(1H,3H)-dione (3f): Gray solid, yield: 53%. ^{1}H NMR (400 MHz, $CDCl_3$): δ = 9.96 (s, 1H), 7.92 (d, J = 2.3 Hz, 1H), 7.41 (dd, J = 8.6, 2.4 Hz, 1H), 6.88 (d, J = 8.6 Hz, 1H), 1.71 (s, 9H). ^{13}C NMR (100 MHz, $CDCl_3$): δ = 162.1, 151.8, 135.5, 133.5, 127.3, 126.7, 117.1, 114.5, 61.5, 28.8.

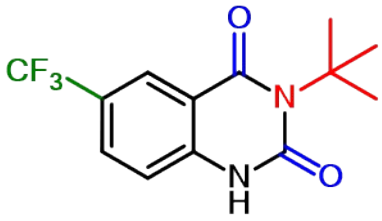

3-(tert-butyl)-6-(trifluoromethyl)quinazoline-2,4(1H,3H)-dione (3g): Brown solid, yield: 74%. ^{1}H NMR (400 MHz, $CDCl_3$): δ = 10.51 (s, 1H), 8.25 (s, 1H), 7.71 (dd, J = 8.5, 1.5 Hz, 1H), 7.69 (d, J = 8.3 Hz, 1H), 1.73 (s, 9H). ^{13}C NMR (100 MHz, $CDCl_3$): δ = 162.2, 152.1, 139.4, 130.0 (J = 3.4 Hz), 125.1, 124.4 (J = 33.5 Hz), 124.0 (J = 270.1

Hz), 115.8, 113.7, 61.8, 28.8.

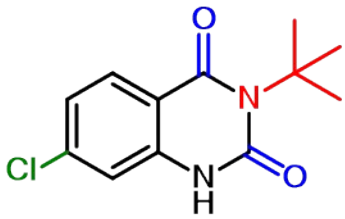

3-(tert-butyl)-7-chloroquinazoline-2,4(1H,3H)-dione (3h): Yellow solid, yield: 94%. ^{1}H NMR (400 MHz, $CDCl_3$): δ = 9.78 (m, 1H), 7.88 (d, J = 8.5 Hz, 1H), 7.06 (dd, J = 8.5, 1.9 Hz, 1H), 6.92 (t, J = 1.5 Hz, 1H), 1.71 (s, 9H). ^{13}C NMR (100 MHz, $CDCl_3$): δ = 162.5, 151.7, 139.5, 137.8, 128.7, 122.4, 114.4, 112.8, 61.4, 28.9.

Compound 3a

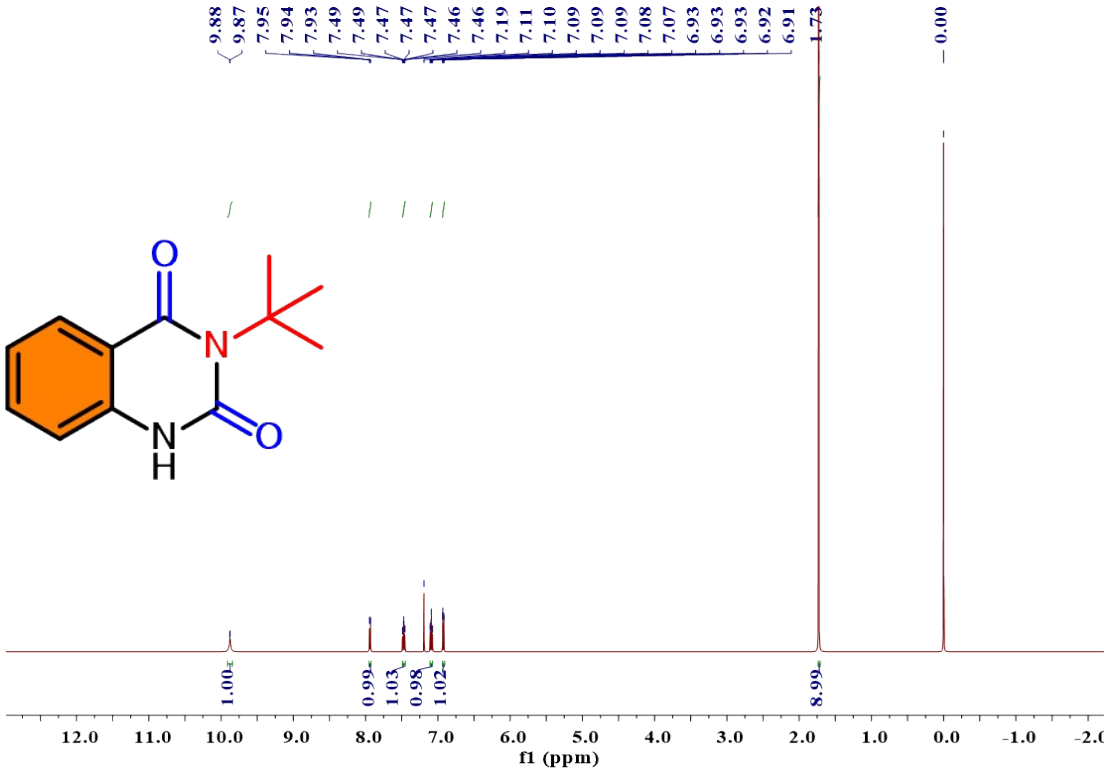
9.88
9.87
7.95
7.94
7.93
7.49
7.49
7.47
7.47
7.47
7.46
7.46
7.19
7.11
7.10
7.09
7.09
7.09
7.08
7.07
6.93
6.93
6.93
6.92
6.91
1.73
0.00
O
N
N
H
O
1.00
0.99
1.03
0.98
1.02
8.99
12.0
11.0
10.0
9.0
8.0
7.0
6.0
5.0
4.0
3.0
2.0
1.0
0.0
-1.0
f1 (ppm)

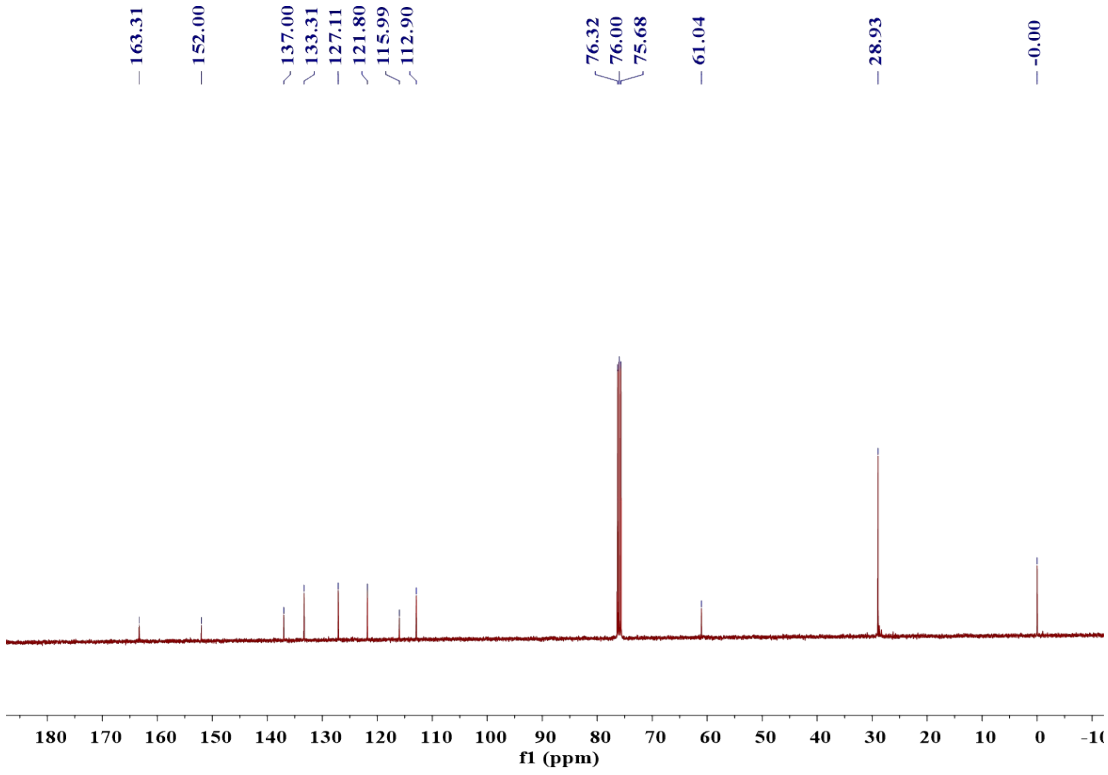
163.31
152.00
137.00
133.31
127.11
121.80
115.99
112.90
76.32
76.00
75.68
61.04
28.93
-0.00
180
170
160
150
140
130
120
110
100
90
80
70
60
50
40
30
20
10
0
f1 (ppm)

Compound 3b

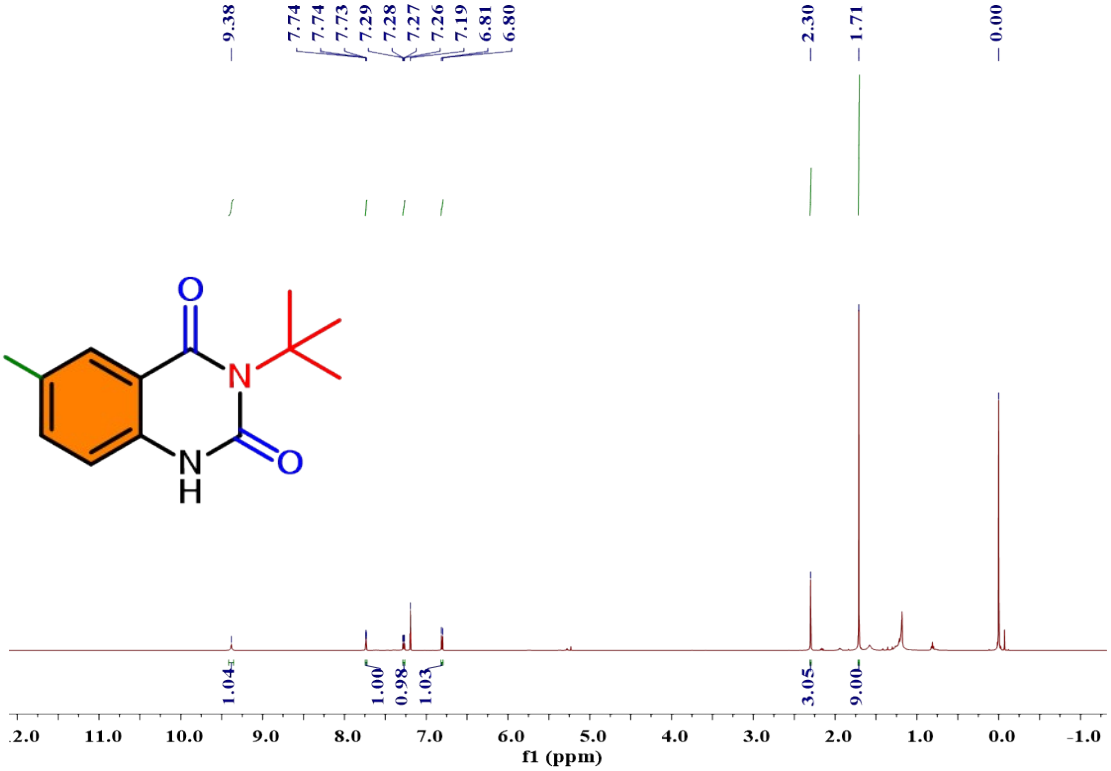
9.38
7.74
7.74
7.73
7.29
7.28
7.27
7.26
7.19
6.81
6.80
2.30
1.71
0.00
O
N
N
H
O
1.04
1.00
0.98
1.03
3.05
9.00
f1 (ppm)

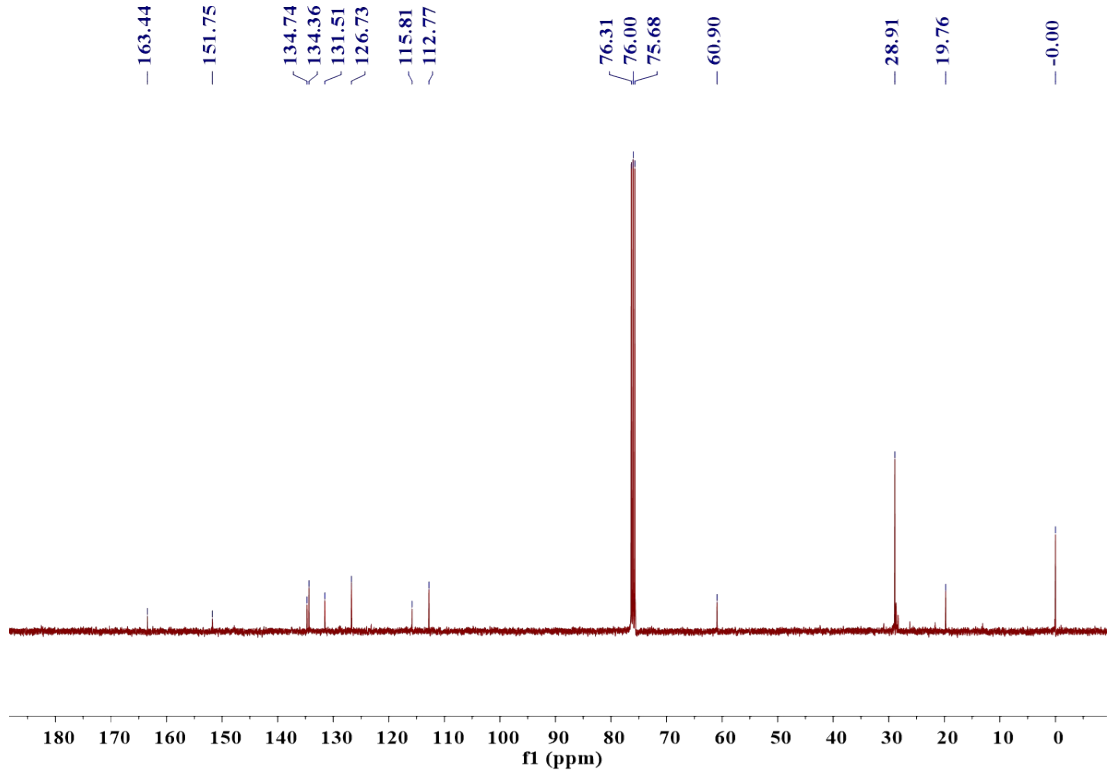
163.44
151.75
134.74
134.36
131.51
126.73
115.81
112.77
76.31
76.00
75.68
60.90
28.91
19.76
-0.00
f1 (ppm)

Compound 3c

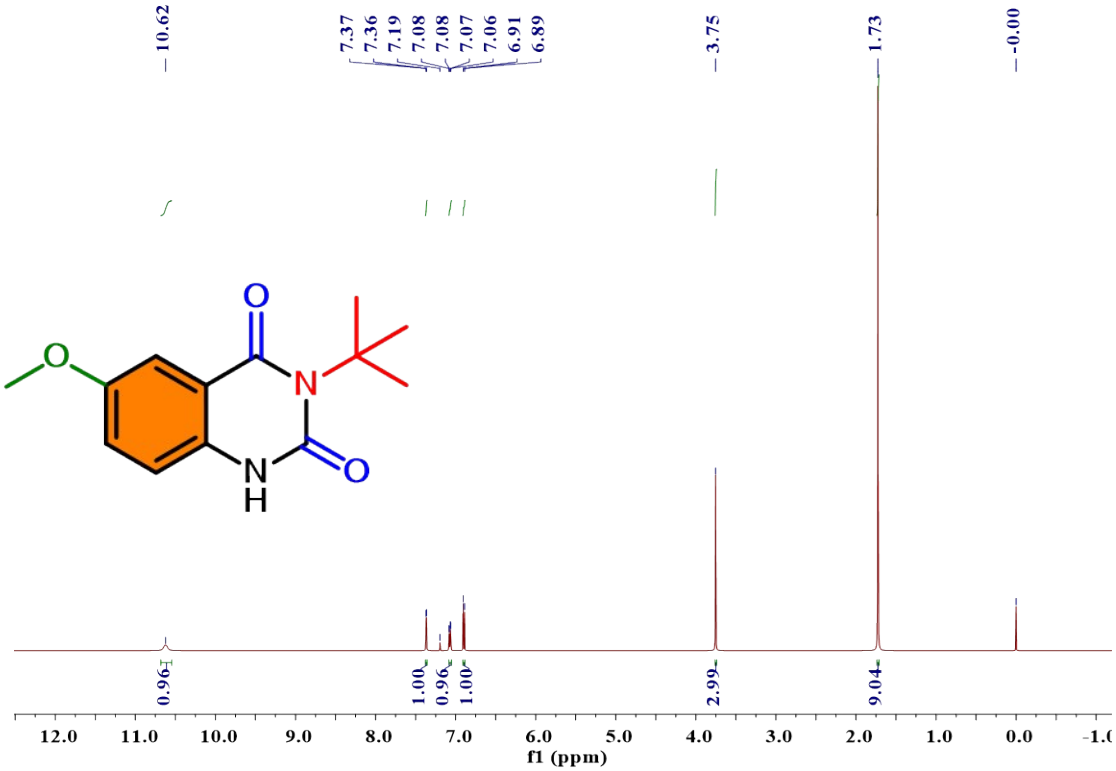
10.62
7.37
7.36
7.19
7.08
7.08
7.07
7.06
6.91
6.89
3.75
1.73
0.00
O
O
N
N
H
O
0.96
1.00
0.96
1.00
2.99
9.04
f1 (ppm)

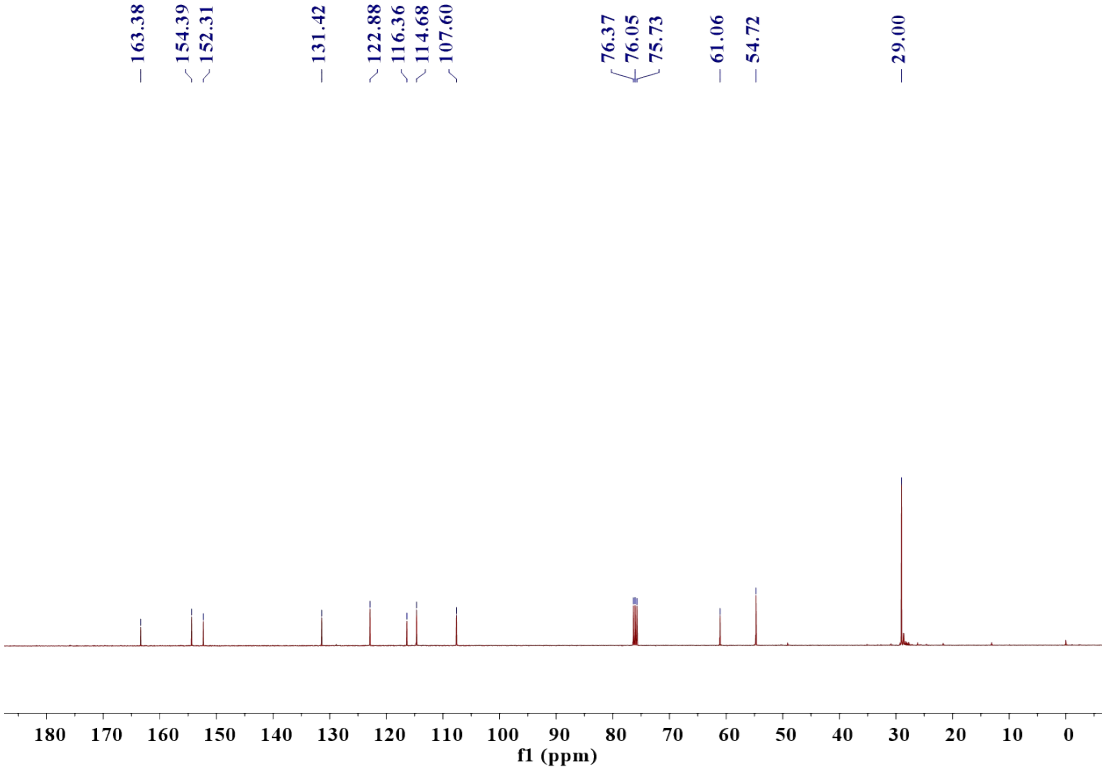
163.38
154.39
152.31
131.42
122.88
116.36
114.68
107.60
76.37
76.05
75.73
61.06
54.72
29.00
f1 (ppm)

Compound 3d

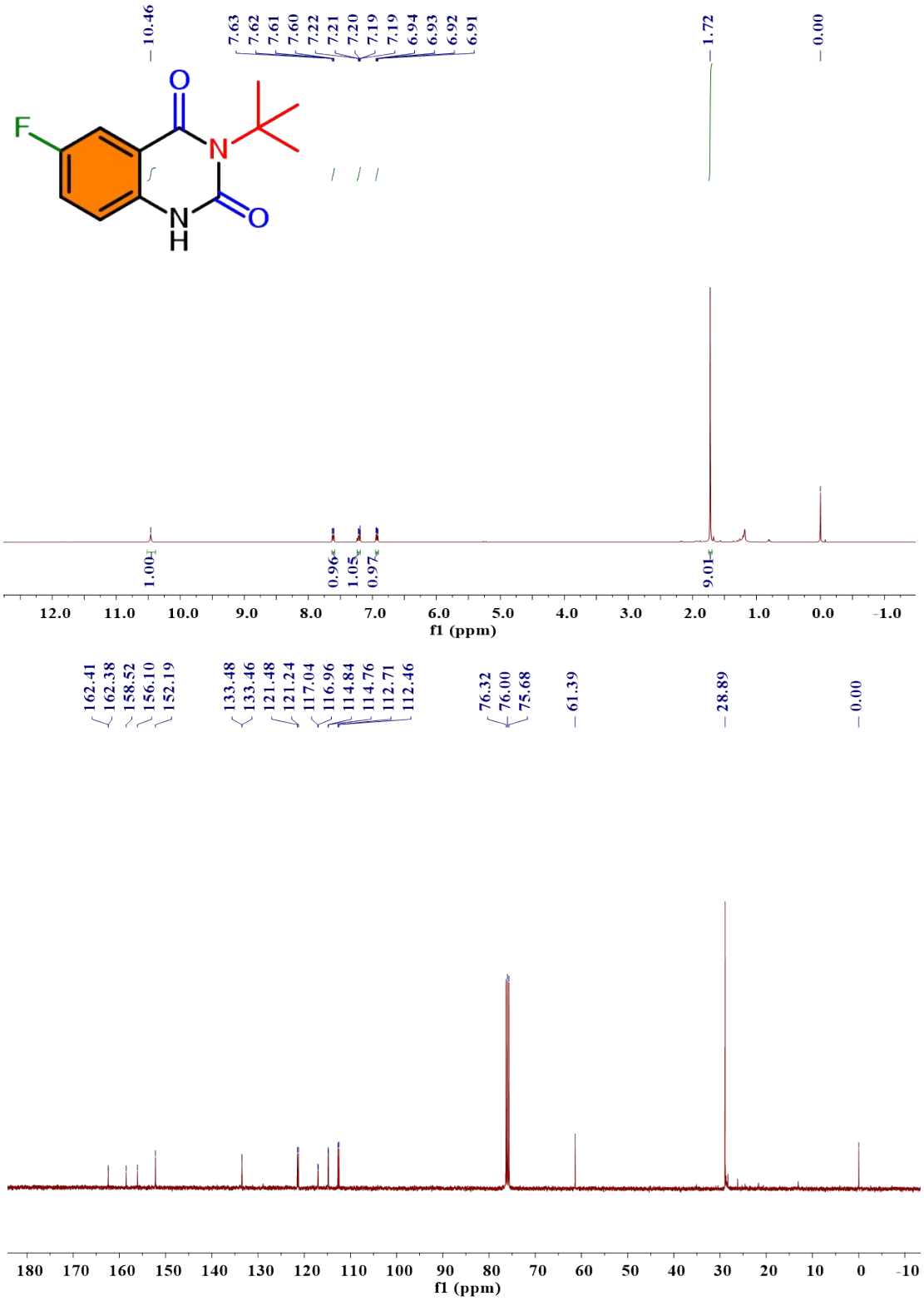
10.46
7.63
7.62
7.61
7.60
7.22
7.21
7.20
7.19
7.19
6.94
6.93
6.92
6.91
1.72
0.00
F
O
N
O
N
H
1.00
0.96
1.05
0.97
9.01
12.0
11.0
10.0
9.0
8.0
7.0
6.0
5.0
4.0
3.0
2.0
1.0
0.0
-1.0
f1 (ppm)
162.41
162.38
158.52
156.10
152.19
133.48
133.46
121.48
121.24
117.04
116.96
114.84
114.76
112.71
112.46
76.32
76.00
75.68
61.39
28.89
0.00
180
170
160
150
140
130
120
110
100
90
80
70
60
50
40
30
20
10
0
-10
f1 (ppm)

Compound 3e

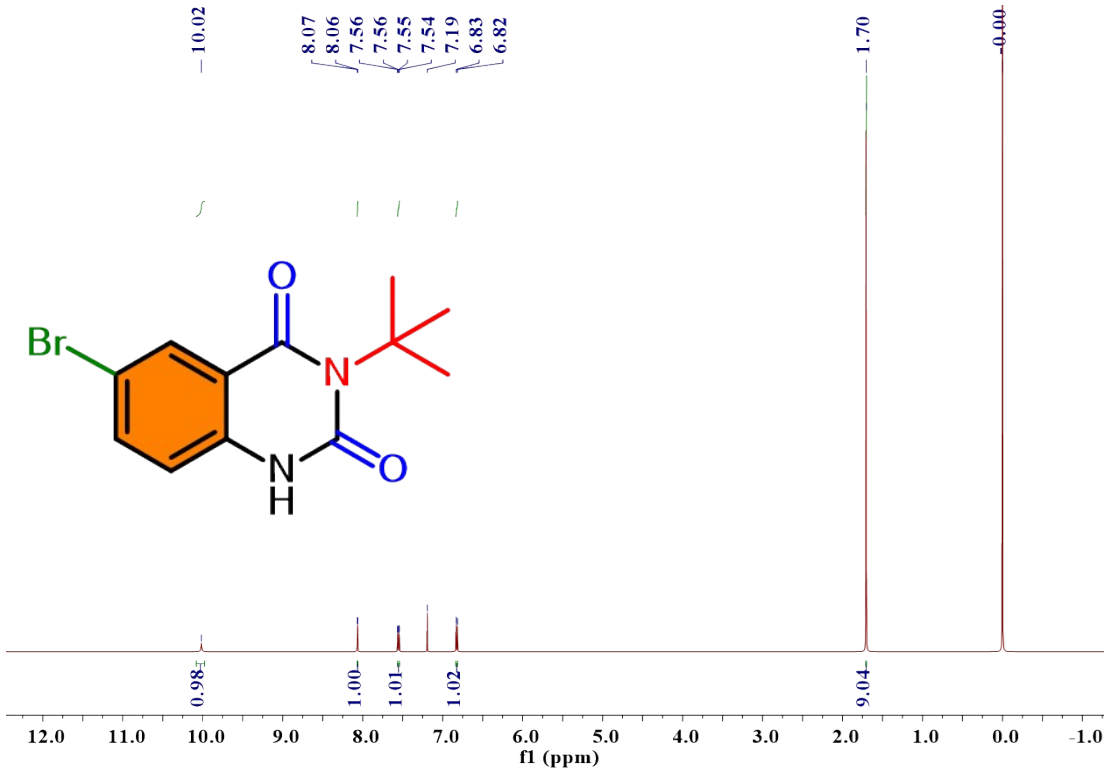
10.02
8.07
8.06
7.56
7.55
7.54
7.19
6.83
6.82
1.70
0.00
Br
O
N
N
H
O
0.98
1.00
1.01
1.02
9.04
12.0
11.0
10.0
9.0
8.0
7.0
6.0
5.0
4.0
3.0
2.0
1.0
0.0
-1.0
f1 (ppm)

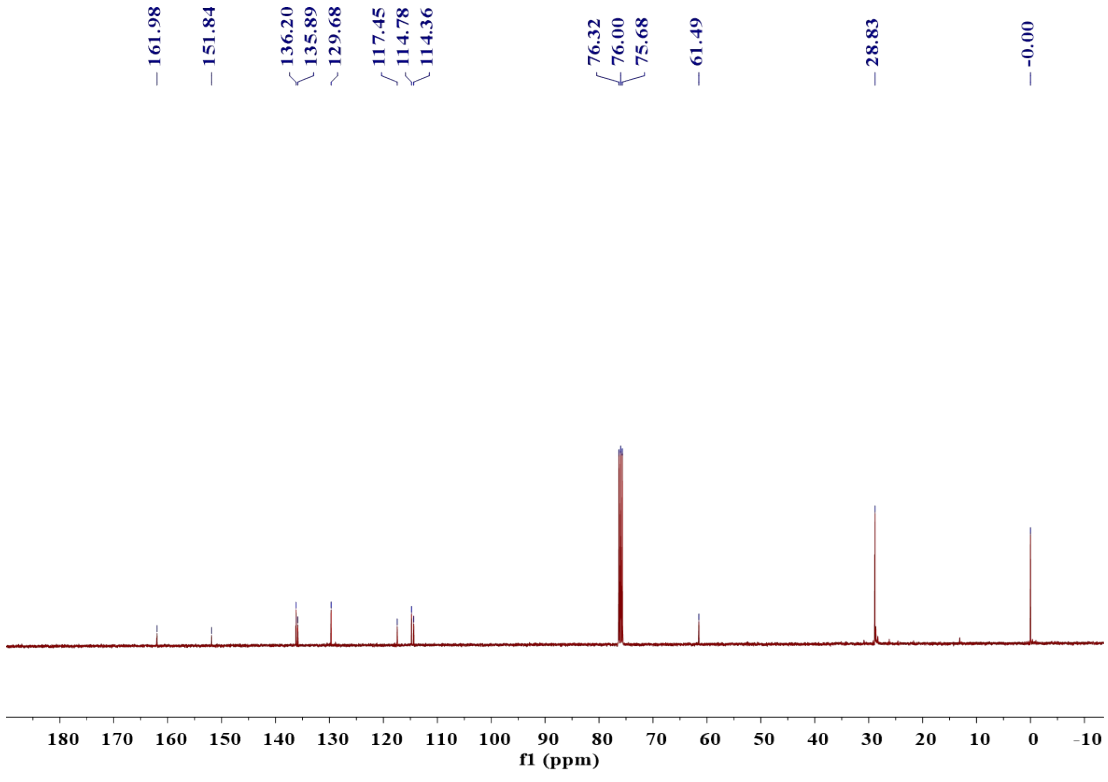
161.98
151.84
136.20
135.89
129.68
117.45
114.78
114.36
76.32
76.00
75.68
61.49
28.83
-0.00
180
170
160
150
140
130
120
110
100
90
80
70
60
50
40
30
20
10
0
-10
f1 (ppm)

Compound 3f

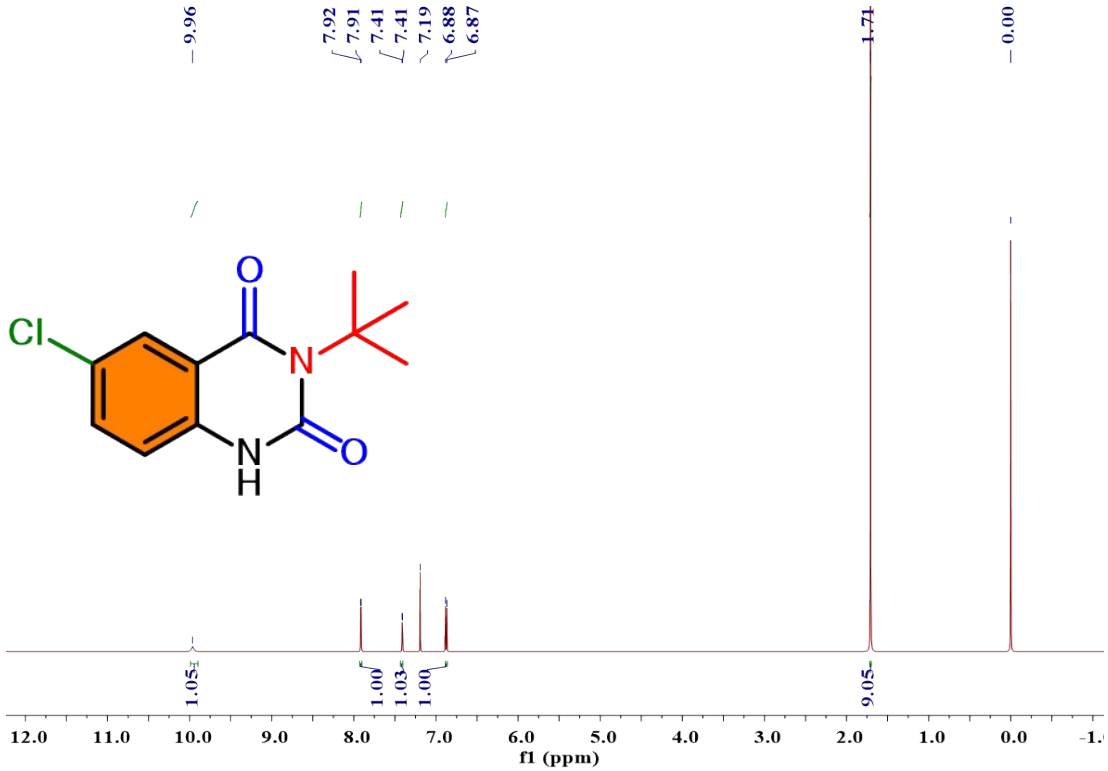
9.96
7.92
7.91
7.41
7.41
7.19
6.88
6.87
1.71
0.00
Cl
O
N
N
H
O
1.05
1.00
1.03
1.00
9.05
12.0
11.0
10.0
9.0
8.0
7.0
6.0
5.0
4.0
3.0
2.0
1.0
0.0
f1 (ppm)

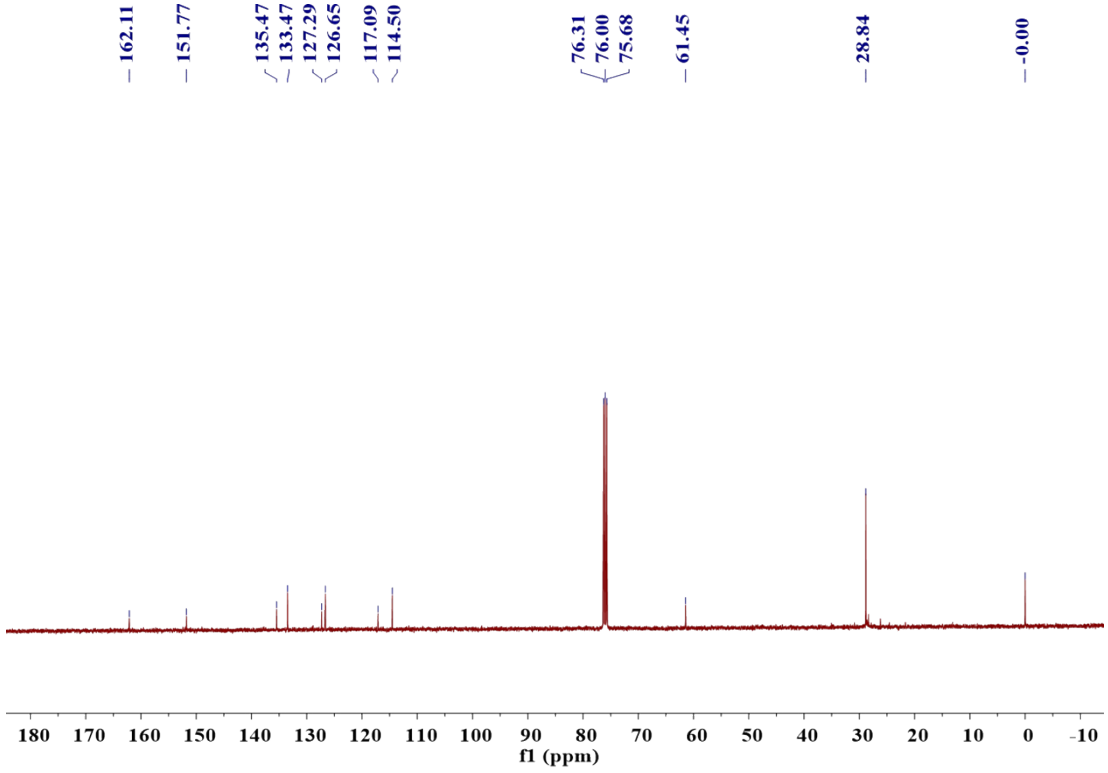
162.11
151.77
135.47
133.47
127.29
126.65
117.09
114.50
76.31
76.00
75.68
61.45
28.84
-0.00
180
170
160
150
140
130
120
110
100
90
80
70
60
50
40
30
20
10
0
-10
f1 (ppm)

Compound 3g

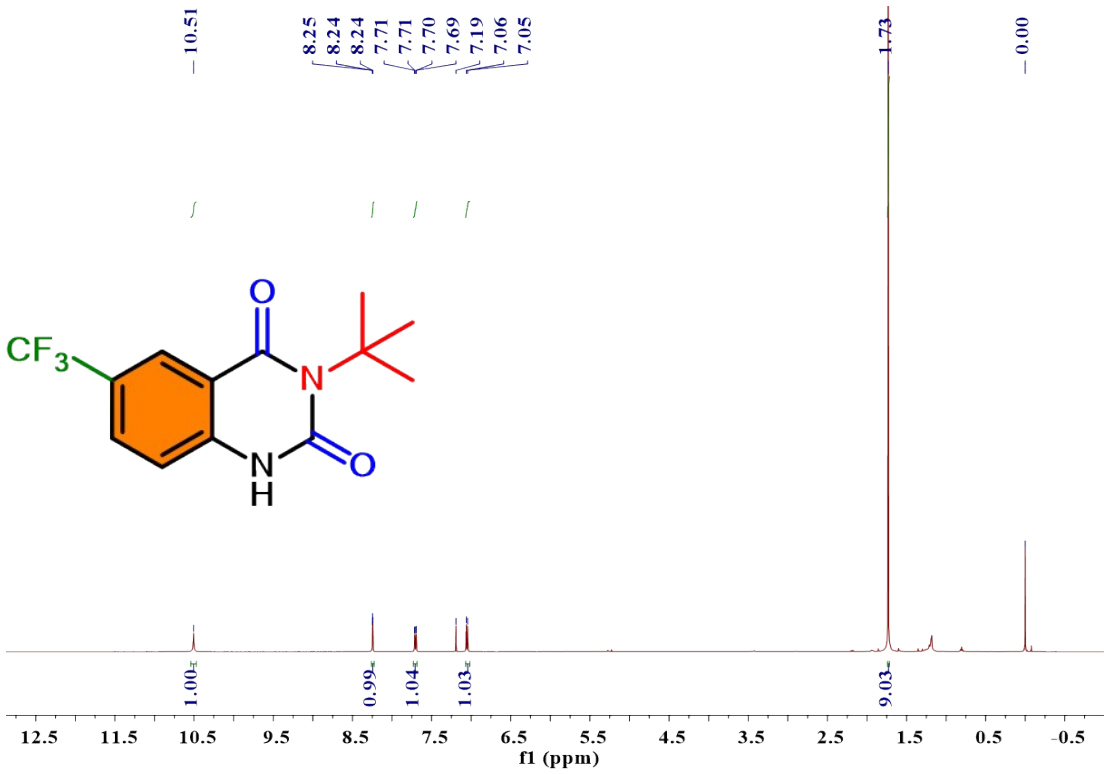
10.51
8.25
8.24
8.24
7.71
7.71
7.70
7.69
7.19
7.06
7.05
1.73
0.00
O
CF3
N
N
H
O
1.00
0.99
1.04
1.03
9.03
12.5 11.5 10.5 9.5 8.5 7.5 6.5 5.5 4.5 3.5 2.5 1.5 0.5 -0.5
f1 (ppm)

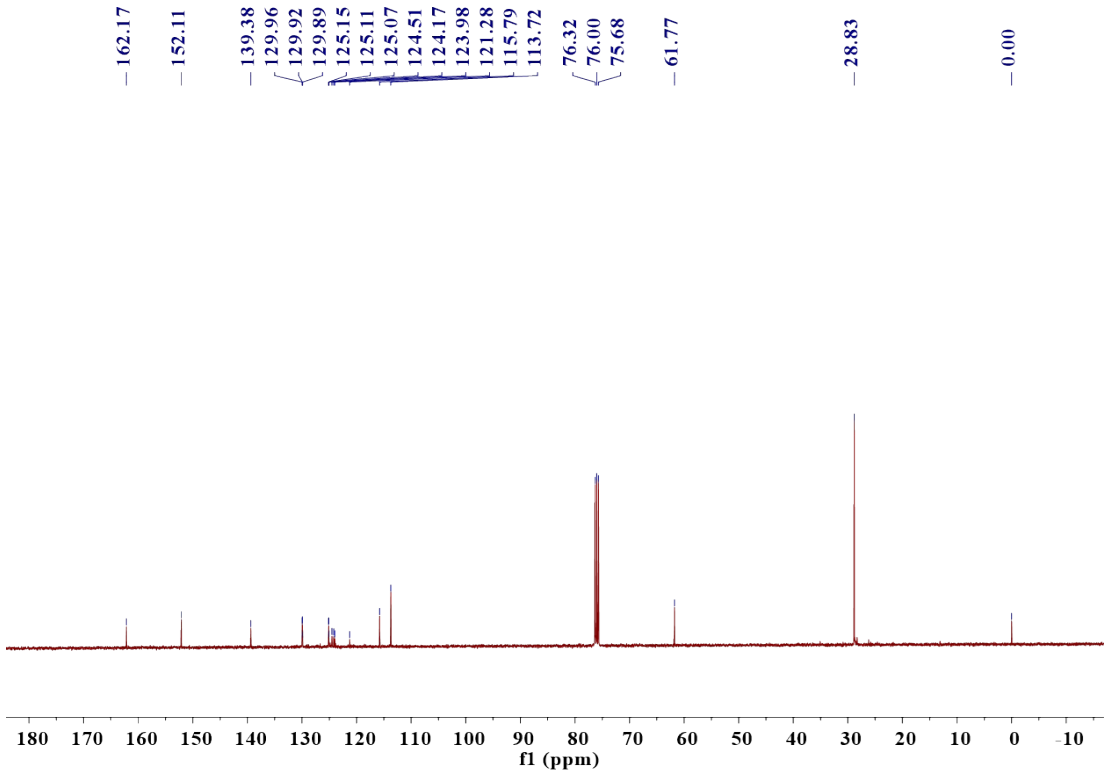
162.17
152.11
139.38
129.96
129.92
129.89
125.15
125.11
125.07
124.51
124.17
123.98
121.28
115.79
113.72
76.32
76.00
75.68
61.77
28.83
0.00
180 170 160 150 140 130 120 110 100 90 80 70 60 50 40 30 20 10 0 -10
f1 (ppm)

Compound 3h

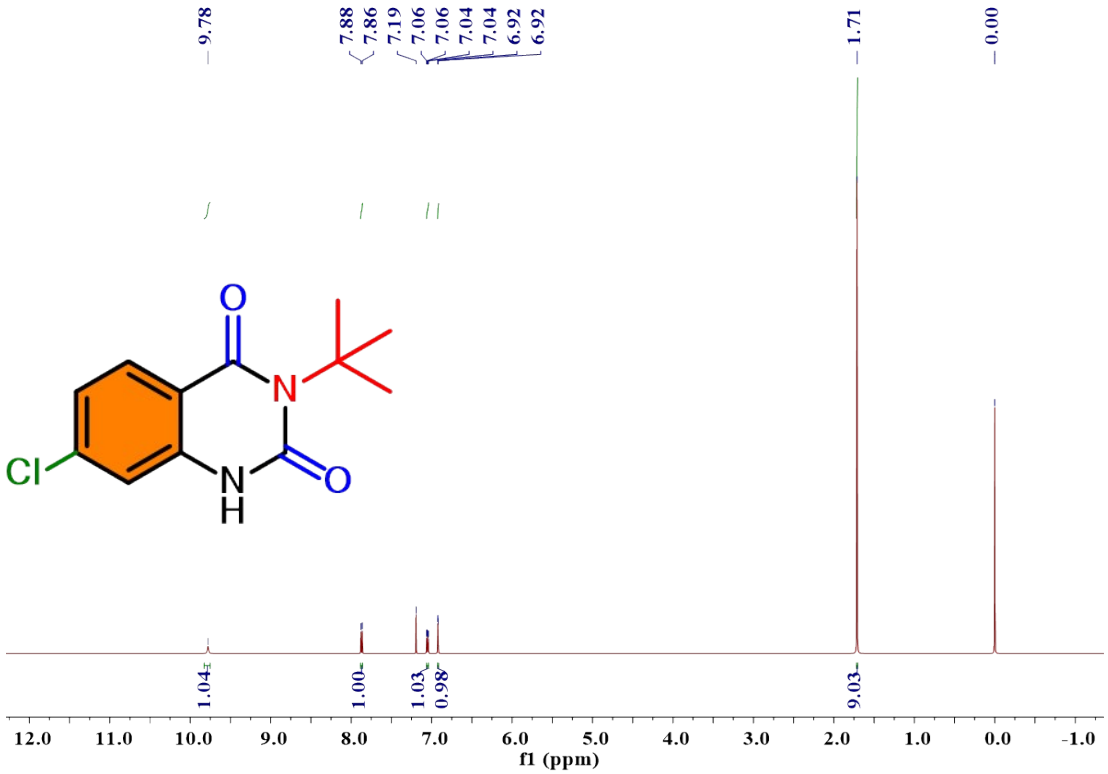
9.78
7.88
7.86
7.19
7.06
7.06
7.04
7.04
6.92
6.92
1.71
0.00
O
N
Cl
N
H
O
1.04
1.00
1.03
0.98
9.03
12.0
11.0
10.0
9.0
8.0
7.0
6.0
5.0
4.0
3.0
2.0
1.0
0.0
-1.0
f1 (ppm)

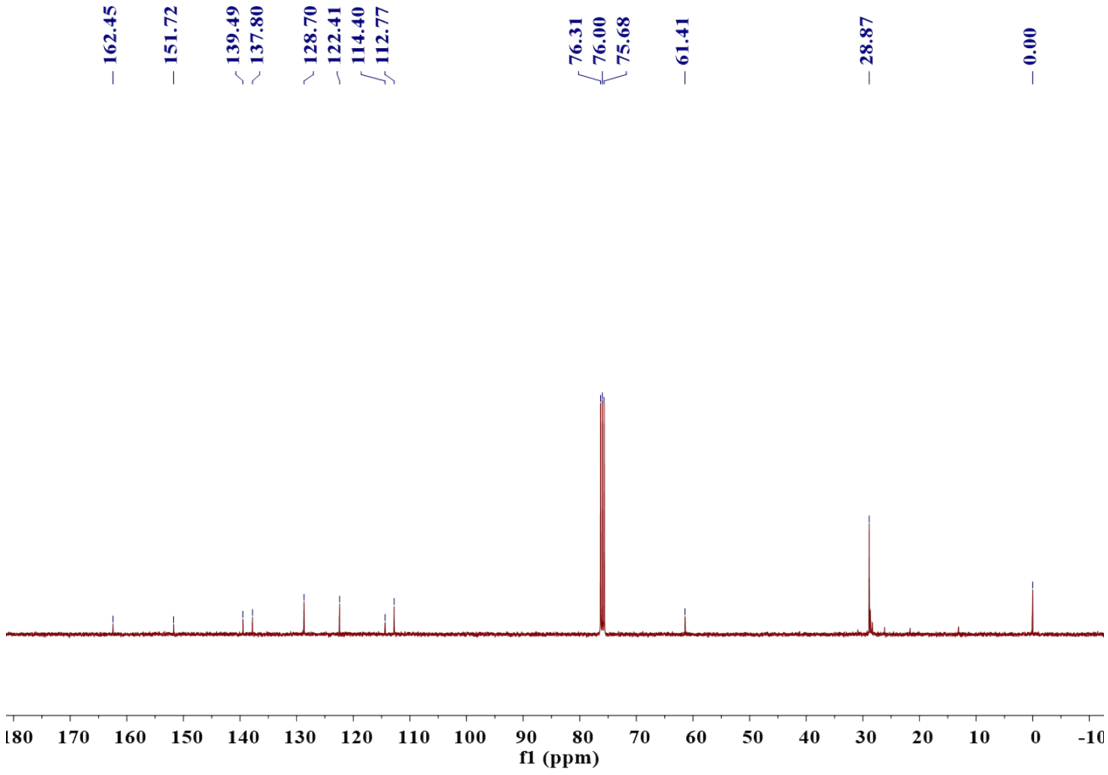
162.45
151.72
139.49
137.80
128.70
122.41
114.40
112.77
76.31
76.00
75.68
61.41
28.87
0.00
180
170
160
150
140
130
120
110
100
90
80
70
60
50
40
30
20
10
0
-10
f1 (ppm)

1 Y. Qian, Y. Han, X. Zhang, G. Yang, G. Zhang and H.-L. Jiang, Computation-based regulation of excitonic effects in donor-acceptor covalent organic frameworks for enhanced photocatalysis. *Nat. Commun.,* 2023**, 14**, 3083.

2 D. Zhu, J.-J. Zhang, X. Wu, Q. Yan, F. Liu, Y. Zhu, X. Gao, M. M. Rahman, B. I. Yakobson, P. M. Ajayan and R. Verduzco, Understanding fragility and engineering activation stability in two-dimensional covalent organic frameworks. *Chem. Sci.,* 2022**, 13**, 9655-9667.

3 N. Lopatik, A. De, S. Paasch, A. Schneemann and E. Brunner, High-field and fast-spinning 1H MAS NMR spectroscopy for the characterization of two-dimensional covalent organic frameworks. *Phys. Chem. Chem. Phys.,* 2023**, 25**, 30237-30245.

4 P. Mampuys, H. Neumann, S. Sergeyev, R. V. A. Orru, H. Jiao, A. Spannenberg, B. U. W. Maes and M. Beller, Combining Isocyanides with Carbon Dioxide in Palladium-Catalyzed Heterocycle Synthesis: N3-Substituted Quinazoline-2,4(1H,3H)-diones via a Three-Component Reaction. *ACS Catal.,* 2017**, 7**, 5549-5556.

5 G. Wang, Y. Gan and Y. Liu, Nickel-Catalyzed Direct Coupling of Allylic Alcohols with Organoboron Reagents. *Chinese J. Chem.,* 2018**, 36**, 916-920.

6 B. Guo, H.-Y. Li, J.-Y. Chen, D. J. Young, J.-P. Lang and H.-X. Li, Conjugated nanoporous polycarbazole bearing a cobalt complex for efficient visible-light driven hydrogen evolution. *New J. Chem.,* 2020**, 44**, 8736-8742.

7 P. Xu, F. Wang, T.-Q. Wei, L. Yin, S.-Y. Wang and S.-J. Ji, Palladium-Catalyzed Incorporation of Two C1 Building Blocks: The Reaction of Atmospheric CO_2 and Isocyanides with 2-Iodoanilines Leading to the Synthesis of Quinazoline-2,4(1H,3H)-diones. *Org. Lett.,* 2017**, 19**, 4484-4487.

8 S. Ren, S. Lin, Z. Ren, M. Wang, Y. Yang, H.-T. Tang, P. Chen, L. Zhou and Y.-M. Pan, Single-Site Palladium "Microreactor" for Carbon Dioxide Coupling/Cyclization Reactions. *ACS Sustainable Chem. Eng.,* 2025**, 13**, 2001-2010.

9 H. Pan, Z. Li, Q. Ma, Y. Zhang, Y. Zheng and Y. Gao, Cobalt catalyst encapsulated by N-doped carbon for selective hydrogenation of aldehyde to alcohol. *Mol. Catal.,* 2024**, 553**, 113752.

10 Y. Liang, K.-Z. Xu, P.-B. Chen, P. Fang, J. Huang and Y.-M. Pan, Sustainable Synthesis of Quinazolinones Through Boiler Flue Gas CO_2 Utilization Via Pd@POP-1 Catalyst Under Mild Conditions. *Adv. Synth. Catal.,* 2025**, 367**, e202500238.

11 Y. Wu, X. Feng, Q. Zhai, H. Wang, H. Jiang and Y. Ren, Metal–Organic Framework Surface Functionalization Enhancing the Activity and Stability of Palladium Nanoparticles for Carbon–Halogen Bond Activation. *Inorg. Chem.,* 2022**, 61**, 6995-7004.